Contract No. 218696-ECONAM

Electromagnetic Characterization Of NAnostructured Materials

Monograph on electromagnetic characterization of nanostructured metamaterials

DELIVERABLE D4.5.1

Due date of deliverable: T0+35 months

Actual delivery date: March 7, 2011

Leading contractors: Aalto, VI

Contributions also from QUB, KIT, U. Glasgow, ITAE, and FORTH

Abstract

This document is a self-standing and complete review which combines a series of analytical overviews and recommendations produced by the ECONAM CSA project during its full duration. The results are presented as a coherent text which can be used as a tutorial and reference source primarily for non-specialists in electromagnetic characterization of materials. More complete and detailed information for specialists can be found on the ECONAM project web site.

Contents

Chapter 1

Introduction

1.1 Nanostructured electromagnetic materials and metamaterials

The design and manufacturing of nanostructured materials has been made possible thanks to progress made in nanotechnologies, material science and electrical engineering. With the help of advanced bottom-up manufacturing techniques, a large number of micrometer scale designs can now being scaled down to nanometer scale and therefore completely new optical materials can be created and investigated. Majority of new nanostructured materials for electromagnetic applications refers to so-called *metamaterials* which exhibit exceptional properties, defined by their geometrical nanostructures. In the literature and on the Internet there are many definitions of metamaterials, which usually stress their unusual electromagnetic properties. Perhaps in the most generic way, metamaterial can be defined as an arrangement of artificial structural elements, designed to achieve advantageous and unusual electromagnetic properties. The concept of material implies homogeneity, i.e. the distance between elements should be small enough. If a metamaterial is a periodical structure, the lattice constants should be considerably smaller than the wavelength in the medium. This distinguishes metamaterials from so-called photonic crystals which are discussed below and from so-called frequency-selective surfaces which are surface analogues of photonic crystals. These are periodic structures whose useful and unusual electromagnetic properties originate mainly from their internal periodicity. In contrast to photonic crystals and frequency selective surfaces, metamaterials possess their properties due to specific electromagnetic response of their "artificial molecules" and not due to specific distances between them (the importance has only the smallness of these distances). Furthermore, the electromagnetic properties of "molecules" are determined not only by their chemical composition, but their geometrical shape plays an important and in most cases the decisive role. The chemical composition is usually chosen so that the response of the inclusion to electromagnetic waves is high (conductive materials, high permittivity materials, ferromagnetic materials) and losses are reasonably small. Specific engineered properties are designed primarily by choosing the inclusions shape and their mutual arrangement.

The research and engineering tools needed to create metamaterials include electromagnetic modelling, geometry and property design, manufacturing, and structural and

electron microscopy characterization at the nanoscale. The final and critical stage of design of new materials for radio, microwave, and optical applications is *electromagnetic characterization*, that is, measurement of electromagnetic properties of material samples.

The research and engineering tools needed to create metamaterials include electromagnetic modelling, geometry and property design, manufacturing, and structural and electron microscopy characterization at the nanoscale. The final and critical stage of design of new materials for radio, microwave, and optical applications is *electromagnetic characterization*, that is, measurement of electromagnetic properties of material samples.

This overview is aimed to help the reader to learn more about the place of metamaterials among other nanostructures and especially about their electromagnetic characterization, which represents a fundamental problem of the modern electromagnetic science. Electromagnetic properties of nanostructured metamaterials are determined by the shape of the constituent nanoinclusions, by their concentration, by their geometric arrangement and by the material parameters of their constituents. Due to this highly increased complexity the electromagnetic characterization of metamaterials has become a branch of science in itself. Effective material parameters are often extracted from numerically simulated or experimentally measured reflection and transmission coefficients. Traditionally, these effective parameters are the basic phenomenological material parameters: permittivity and permeability. In the case of natural materials (and also for composite bulk media which cannot be referred to metamaterials but behave as effectively continuous structures) these parameters usually give a good description of the electromagnetic behavior. But metamaterials cannot always be characterized in this simple and traditional way. Many metamaterials need more parameters for their characterization and, in general, the physical meaning and practical applicability of material parameters is to be carefully examined before these parameters can be used in design of various applications.

An introductory text about metamaterials can be found in [1].

1.2 Electromagnetic waves in materials

Electromagnetic fields in materials are governed by the macroscopic Maxwell equations

$$\nabla \times \mathbf{E} = -\frac{\partial \mathbf{B}}{\partial t}, \qquad \nabla \times \mathbf{H} = \frac{\partial \mathbf{D}}{\partial t} + \mathbf{J}^{\text{ext}}. \tag{1.1}$$

In these equations $\mathbf{E}$ and $\mathbf{H}$ are the macroscopic electric and magnetic fields, $\mathbf{D}$ and $\mathbf{B}$ are the corresponding flux vectors, and $\mathbf{J}^{\text{ext}}$ is the external (source) electric current density. The simplest field solutions in homogeneous source-free regions are plane waves.

For time-harmonic fields we can replace time derivatives by simple multiplication and write, for the time dependence in from $\exp(j\omega t)$,

$$\nabla \times \mathbf{E} = -j\omega \mathbf{B}, \qquad \nabla \times \mathbf{H} = j\omega \mathbf{D} + \mathbf{J}^{\text{ext}}. \tag{1.2}$$

A time-harmonic plane wave propagating along the z-axis with the wave number q is described as $A\exp(j\omega t - jqz)$, where A is the wave phasor (complex amplitude) which can refer to any component of the field vectors $\mathbf{E}, \mathbf{H}, \mathbf{D}$ or $\mathbf{B}$, ω is the frequency, and $j = \sqrt{-1}$. The real time-dependent field which is physically observable is calculated as

$$E(t,z) = \mathrm{Re}[A\exp(j\omega t - jqz)] = |A|\cos[\omega t - qz + \arg(A)]. \tag{1.3}$$

Since the factor $\exp(j\omega t)$ is common for all field vectors, it is usually omitted. The time dependence $\exp(j\omega t)$ is usually adopted by electrical engineers, while physicists usually prefer the choice of $\exp(-i\omega t)$ (where the imaginary unit is denoted as i). Then the physically observable field of the plane wave is calculated as $\mathrm{Re}[A\exp(-i\omega t + iqz)]$. If a wave propagates obliquely with respect to the coordinate axis, one presents the plane wave through the wave vector $\mathbf{q}$. Then for a point with the radius-vector $\mathbf{r}$ one has $A\exp(-j\mathbf{q}\cdot\mathbf{r})$ in the "engineering notation" and $A\exp(i\mathbf{q}\cdot\mathbf{r})$ in the "physical notation".

Plane waves which can exist in a given medium in the absence of sources are called the medium eigenmodes. The concept of eigenmodes is also valid for periodical structures (lattices) as it is explained below. In the general case the time-harmonic wave field created by a given set of sources can be presented as a combination of plane waves (eigenmodes). This combination (which is rarely discrete, more often it is continuous) is called the spatial spectrum. An electromagnetic pulse can be presented through time harmonics as its frequency spectrum. So, in the general case the time-varying electromagnetic field is the double spectrum comprising both frequency spectrum and the spatial spectrum – spectrum of eigenmodes.

From the Maxwell equations it follows that a plane electromagnetic wave incident on a half-space filled with a continuous material partially refracts into it and partially reflects. The refracted and reflected waves are also plane waves. The incidence of a plane wave on a half-space is one of the simplest boundary problems. The next grade of complexity for the boundary problem is the case of a plane wave incident on a planar layer. In this case the refracted wave experiences multiple internal reflections in the layer and partially penetrates behind the layer. The wave behind the layer is called *transmitted wave*, and it is also a plane wave as well as all partial waves corresponding to the inner reflection events.

1.3 Why do we need effective material parameters?

The set of macroscopic Maxwell equations (1.2) or (1.1) is incomplete, as there are only two equations for four field vectors. Thus, the macroscopic field equations must be supplemented by *constitutive relations* which model the electromagnetic properties of the medium. The only alternative to this macroscopic description is directly solving the microscopic Maxwell equations, where each and every electron should be accounted for separately. Of course, this is absolutely not realistic in any practically interesting situation when we deal with *material* samples containing huge numbers of molecules (or small particles, in the case of metamaterials and other nanostructures).

Introduction of effective electromagnetic parameters of a material is called *homogenization*. In this approach a heterogeneous structure is replaced by an effectively homogeneous one. Any homogenization theory is an approximation, because it employs a finite number of parameters to describe samples with huge numbers of molecules (for artificial materials – inclusions). In the case of metamaterials the response of these inclusions is dispersive, i.e., the inclusions respond to a pulse excitation with some time delay. In

terms of effective parameters for time-harmonic fields, this means that the parameters (permittivity, permeability,...) significantly depend on the frequency of excitation. Even if a direct "brute force" solution of the electrodynamic problem for an array comprising a huge number of inclusions would be feasible, this still would not give any hint on what will happen if we change the sample shape, for instance. To design a new electromagnetic material, the researcher should find the optimal shape and chemical content of inclusions, their optimal size and mutual arrangement, the optimal distance between them, etc. This means that many realizations of the material should be considered before the optimal design is obtained. The homogenization allows one to avoid the exact simulation of each realization, each size and each shape of material samples.

Homogenization means that material parameters of an artificial material are obtained and constitutive relations in which these parameters enter are known. Then one can analytically solve macroscopic Maxwell's equations complemented with these constitutive relations. This solution for bulk materials is usually done assuming the infinite space filled with the material in the absence of sources. This way one determines all the eigenwaves that can exist in the infinite artificial medium. By enforcing the appropriate boundary conditions, the amplitudes of these eigenmodes are found for a finite-size sample of the medium. For nanostructured materials in many practically relevant situations samples are parallel-plate layers. If a nanostructured layer can be considered as a layer of an effectively bulk medium, the field inside it can be expressed as a superposition of the medium eigenmodes. The amplitudes of the eigenmodes used to decompose the scattered fields (usually reflected and transmitted plane waves) can be obtained, and a solution to the entire electromagnetic problem can be found. However, the approach based on the bulk material eigenmodes cannot be applied to artificial "surface materials" (or *sheets*) where the number of inclusions across the layer is small, which is especially true for a monolayer (a single grid of nanoinclusions on a dielectric substrate). For such structures one needs to introduce special material parameters relevant for an "artificial surface" (which is usually called *metasurface* if the constitutive elements possess resonant response). However, in any case the knowledge of material parameters is an obvious pre-requisite for solving the electrodynamic boundary problem as well as for understanding how the new materials will perform in various device applications.

Bibliography

[1] Nanostructured Metamaterials, Exchange between experts in electromagnetics and materials science, Ed Anne F de Baas, Luxembourg, European Union 2010, ISBN 978-92-79-07563-6

Chapter 2

Complex electromagnetic and optical materials (metamaterials)

In order to understand the modern approaches to electromagnetic characterization of nanostructured materials, we need to know some basic concepts of electromagnetics of materials, discussed in this chapter.

2.1 Effectively homogeneous bulk materials

2.1.1 Homogeneous and effectively homogeneous magneto-dielectric materials

The simplest type of isotropic homogeneous media is the vacuum. The constitutive relations in the vacuum are expressed by the basic linear relations

$$\mathbf{D}(r,t) = \varepsilon_0 \mathbf{E}(r,t), \quad \mathbf{B}(r,t) = \mu_0 \mathbf{H}(r,t), \tag{2.1}$$

where the universal physical constants $\varepsilon_0 = 8.85418782 \cdot 10^{-12}$ F/m and $\mu_0 = 4 \cdot 10^{-7}$ H/m are called the free space permittivity and permeability, respectively.

Vast majority of natural substances are electrically neutral at the macroscopic level. Even at the scale of one nanometer the electric charges in them are not separated. Only permanent magnets and electrets are known as exceptions. Macroscopic electrical neutrality of materials is the consequence of an internal equilibrium in collective interactions of microscopic charges. In good insulators, positive and negative charges in atoms are tightly tied together and immense external energy is necessary to break the bonds. However, when the electromagnetic wave impinges on the sample, external electric and magnetic fields cause oscillatory displacements of charges from their original positions. Effects of local separation of positive and negative charges in the external electric field manifests itself in form of induced electric *dipoles*, and it is called *polarization*.

Several different mechanisms are responsible for polarization phenomena, e.g. electron displacement (dominant in non-polar solid media), polar molecule reorientation, ionization (dominant in plasma), etc. Similar effects caused by magnetic field are called magnetization (magnetic polarization). Presence of dielectric or magnetic materials alters the flux

densities $\mathbf{D}$ and $\mathbf{B}$ due to electric $\mathbf{P}$ and magnetic $\mathbf{M}$ polarizations of the medium unit volume. The constitutive relations of a continuous medium with electric and magnetic properties result from the definitions

$$\mathbf{D}(r,t) = \varepsilon_0 \mathbf{E}(r,t) + \mathbf{P}(r,t), \quad \mathbf{B}(r,t) = \mu_0 \mathbf{H}(r,t) + \mathbf{M}(r,t), \tag{2.2}$$

where $\mathbf{P}(r,t)$ and $\mathbf{M}(r,t)$ usually linearly depend on the fields $\mathbf{E}(r,t)$ and $\mathbf{H}(r,t)$. In majority of electromagnetically isotropic materials, the electric and magnetic responses of the medium can be separated. Then the susceptibilities of the isotropic material exposed to the time-dependent fields can be represented by the following linear relations

$$\mathbf{P}(r,t) = \varepsilon_0 \int_{-\infty}^{t} \kappa_e(r, t-t')\mathbf{E}(r,t')dt', \quad \mathbf{M}(r,t) = \mu_0 \int_{-\infty}^{t} \kappa_m(r, t-t')\mathbf{H}(r,t')dt', \tag{2.3}$$

where the scalar functions $\kappa_{e,m}$ are the electric and magnetic susceptibilities.

The time required to develop material reaction to the electromagnetic field exposure varies, and any response from matter may strongly depend on the frequency. For example, electronic polarization is more sensitive to higher frequencies than ionic polarization, and in artificial materials that are made of macroscopic artificial molecules the response may be very strong at some frequencies in the radio (especially, microwave) range or in the optical range, strongly dependent on the size and shape of the inclusions. The instantaneous polarization at time t is expressed as a convolution over the past history and it has rather complicated form in time domain. On the other hand, since the induced polarization is represented by a convolution in the time domain (2.3), its expression in the frequency domain is reduced to a simple multiplication operation:

$$\mathbf{P}(r,\omega) = \epsilon_0 \tilde{\kappa}_e(r,\omega)\mathbf{E}(r,\omega), \qquad \mathbf{M}(r,\omega) = \mu_0 \tilde{\kappa}_m(r,\omega)\mathbf{H}(r,\omega), \tag{2.4}$$

where $\tilde{\kappa}_{e,m}(\omega)$ are the Fourier transformed kernels $\kappa_{e,m}(t)$. This leads to the material (constitutive) relation between the electric flux density $\mathbf{D}$ and the electric field strength $\mathbf{E}$ and that the magnetic flux density $\mathbf{B}$ and the magnetic field strength $\mathbf{H}$ at frequency ω in the form:

$$\mathbf{D} = \varepsilon_0 \varepsilon(r,\omega)\mathbf{E}, \quad \mathbf{B} = \mu_0 \mu(r,\omega)\mathbf{H} \tag{2.5}$$

with $\varepsilon = 1 + \tilde{\kappa}_e$ and $\mu = 1 + \tilde{\kappa}_m$.

In these equations $\mathbf{E}$ and $\mathbf{H}$ are the so-called complex amplitudes of the *macroscopic* electric and magnetic fields which result from the averaging of the actual (microscopic) electric and magnetic field vectors over the unit cell of the material. This unit cell for simple arrays, such as a simple cubic lattice, includes only one particle forming the material, e.g. one atom or molecule (or an "artificial atom or molecule" of a metamaterial). For complex arrays the unit cell can contain many particles.

Material parameters ε and μ in (2.5) are called relative permittivity and relative permeability, respectively. They can be functions of not only frequency ω, but also of spatial coordinates. However, the latter dependence exists only in inhomogeneous materials with spatially variable macroscopic electromagnetic properties. In homogeneous media the permittivity and permeability are spatially invariant and, therefore, their coordinate dependencies can be dropped.

Now let us consider artificial materials. They operate in the radio, microwave, or optical frequency ranges, where the host materials (as a rule, some natural dielectrics) can be with the highest achievable accuracy considered as electromagnetically continuous media. Incorporating many small inhomogeneities called "inclusions" or particles in such a host material one can obtain artificial dielectrics whose permittivity can be very different from that of the host medium. This is so if the electromagnetic properties (permittivity, conductivity) of inclusions are enough different from that of the background medium. Particles immersed in a homogeneous host material may be arranged in periodic or quasi-periodic lattices, or be randomly dispersed. The response of such *composite medium* to electromagnetic exposure is predominantly determined by the particle polarizations and inter-particle interactions. Thus, the electromagnetic properties of artificial media fundamentally depend on the electrical dimensions of inclusions and the lattice periods as compared with the wavelength of the applied field. When the particle sizes and inter-particle distances are small enough compared to the wavelength, this is the key prerequisite for the possibility of homogenization, i.e. of the representation of the artificial medium as an effectively continuous one (this is the case of "electromagnetic materials").

Most often optically small inclusions behave in the applied electromagnetic field as electric dipoles whose amplitude is proportional to the applied field. If the dipole moment of inclusions in the frequency range of our interest does not experience a resonance and the distances between inclusions are electrically small, the permittivity of the whole composite can be calculated using static *mixing rules*. In the simplest case when the concentration of inclusions is small or the contrast is not high, this effective permittivity is just the averaged value, in which the permittivities of the matrix (host medium) and of particles enter with appropriate weight coefficients, determined by the volume fraction ratio of the inclusions in the composite. Strongly dispersive and resonant dielectric properties of nanostructured materials appear mainly due to non-trivial (e.g., negative) permittivity of the material from which the inclusions are made. The shape and arrangement of inclusions can strongly influence to the resulting ε.

Inclusions can be also made of a natural magnetic, then the composite can possess natural magnetic properties. Magnetic properties of materials are described usually by permeability μ. Most of the current research in metamaterials mainly concerns with the design of magnetic properties using non-magnetic constitutive materials (so-called "artificial magnetism"). This is because nanostructured materials exhibit their useful electromagnetic properties mainly in the optical range where the natural magnetism vanishes, and magnetic response due to complex inclusion shape is the only possibility to realize magnetic properties. This phenomenon of artificial magnetism is a special case of the so-called *weak spatial dispersion*, and it can exist only if the inclusion size is not negligible as compared with the wavelength. In this case one can think about magnetic materials consisting of artificial molecules rather than of artificial atoms, usually arrays of complex-shaped inclusions (such as split metal rings) where circulating conduction or polarization currents are induced in every inclusion by external electromagnetic field. Alternatively, artificial magnetic molecules can be formed by several strongly interacting particles. Still another approach to realizing artificial magnetism is the use of high permittivity small dielectric spheres embedded in a homogeneous dielectric matrix. Due to magnetic Mie resonance mode, a small dielectric sphere under the condition of a high optical contrast can scatter the incident wave as if it were a magnetic dipole scatterer.

In the literature, one can also find a number of attempts to exploit uniform magnetic resonances in nanoinclusions of natural magnetic materials, e.g. ferromagnets and antiferromagnets. These nanostructures operate in the radio frequency range, since in the optical range natural magnetics lose their magnetic properties. In all these cases magnetic materials have a non-trivial permeability, which is dispersive, i.e., strongly depends on the frequency.

2.1.2 Conducting, diamagnetic and paramagnetic materials

In contrast to dielectrics where tightly bound charges experience only displacement in the applied field, in good conductors such as copper or silver, there are conduction electrons that are free to drift in the material. Therefore, external electric field causes directed motion of free electrons along the field, i.e., electric current. In most of good conductors, the current density $\mathbf{J}$ and electric field $\mathbf{E}$ are related by the Ohm law which in its general form can be written as

$$\mathbf{J}(\omega, \mathbf{r}) = \sigma(\omega, \mathbf{r})\mathbf{E}(\omega, \mathbf{r}). \tag{2.6}$$

Here σ is the electric conductivity of the material expressed in Siemens per meter. Conductivity of a material is an intrinsic property of the material determined by mobility of free electrons. The motion of individual conduction electrons is exceedingly complex and is defined by the material microstructure. Conductivity may be anisotropic, i.e., dependent on the current direction. In semiconductors, it is usually a non-linear function of $\mathbf{E}$. The conduction electron mobility is responsible for conductivity of conductors at frequencies below 10 GHz. At higher frequencies, the polarization effects should be taken into account when one calculates σ. Real materials are neither perfect conductors nor insulators, i.e., actual dielectrics have some conductivity whilst conductors demonstrate (at high frequencies) relative permittivity which is different from unity. Both these characteristics can be combined by introducing *complex permittivity* of the material for time harmonic electromagnetic field into a complex permittivity $\varepsilon = \varepsilon' - j\varepsilon''$ for the time dependence $\exp(j\omega t)$ or $\varepsilon = \varepsilon' + i\varepsilon''$ for the time dependence $\exp(-i\omega t)$. In good conductors $\varepsilon'' = \sigma/(\omega\varepsilon_0)$. In many practical situations, it is convenient to use the idealizations of perfect conductor ($\sigma \to \infty$) and perfect (lossless) dielectric ($\sigma = 0$). The criteria of treating the medium as a perfect conductor or a lossless dielectric are inferred from comparison of conduction and displacement current magnitudes.

Permeability of most dielectrics and conductors is very close to unity. However, there are two types of weakly magnetic materials – diamagnetic with $\mu < 1$ and paramagnetic with $\mu > 1$. For example, copper is diamagnetic with $\mu = 0.999991$, whilst aluminium is paramagnetic with $\mu = 1.00002$. Natural magnetics such as ferromagnetic materials have very high permeability at dc ("direct current" at zero frequency), e.g. iron has static permeability $\mu|_{\omega=0} = 5000$. However, already at 1 GHz, permeability of iron falls practically to unity. Permittivity, permeability and conductivity of materials vary significantly with the frequency. However, in many practical applications they may be considered frequency independent until the operating wavelengths remains substantially greater than the characteristic scale of the material microstructure or nanostructure. If the frequencies of electromagnetic fields approach the intrinsic resonances of matter, the characterization of the medium by its static parameters becomes inadequate even for natural materials.

2.1.3 Anisotropic and bianisotropic media

The main distinctive feature of isotropic media is that the electromagnetic response is invariant of the propagation direction and polarization of the electromagnetic field. Therefore the material parameters for isotropic media can be reduced to scalar coefficients (in simple media, permittivity and permeability). Models of isotropic homogeneous media provide valuable insight to the main properties of artificial electromagnetic materials. However, many practical materials are not isotropic while remaining reasonably homogeneous. They are called anisotropic materials. For example, most of known metamaterials are anisotropic as their internal microstructure or nanostructure has certain lattice-like arrangements with distinctive axes directions. This implies that the field orientation with respect to the internal structure affects the medium response. Often the linear relations exist between the four vectors of the electromagnetic fields, and the constitutive relations, introduced in the previous subsection, should be generalized by introducing the medium parameters in the form of the permittivity and permeability tensors.

Another complication, also related to complex geometry of nanostructures is electromagnetic coupling, when electric field applied to a (natural or artificial) molecule excites not only electric dipole moment, but also magnetic dipole moment. Likewise, magnetic field can in the general case excite both magnetic and electric polarizations. Materials with magneto-electric coupling are called *bi-isotropic materials* if their response is isotropic or *bianisotropic materials*, if they are anisotropic. In bianisotropic materials the electric polarization and magnetization can be expressed in the following form:

$$\mathbf{P} = \mathbf{P}_0 + \varepsilon_0 \overline{\overline{\kappa}}_e(\omega) \cdot \mathbf{E} + \sqrt{\varepsilon_0 \mu_0}\, \overline{\overline{\kappa}}_{em}(\omega) \cdot \mathbf{H}, \tag{2.7}$$

$$\mathbf{M} = \mathbf{M}_0 + \mu_0 \overline{\overline{\kappa}}_m(\omega) \cdot \mathbf{H} + \sqrt{\varepsilon_0 \mu_0}\, \overline{\overline{\kappa}}_{me}(\omega) \cdot \mathbf{E}, \tag{2.8}$$

where $\mathbf{P}_0, \mathbf{M}_0$ are the static electric polarization and magnetization which exist in the absence of external alternating fields, e.g., in ferroic and multi-ferroic materials, the dimensionless tensors $\overline{\overline{\kappa}}_{e,m}(\omega)$ are the electric and magnetic susceptibilities of an anisotropic medium, and the dimensionless tensors $\overline{\overline{\kappa}}_{em}$ and $\overline{\overline{\kappa}}_{me}$ describe the electric polarization of a bianisotropic medium induced by a magnetic field or magnetization caused by an electric field. The latter terms describe the linear magneto-electric effect which is observed in several oxide materials as well as in artificial bianisotropic materials which all refer to the class of metamaterials.

Although the polarization and magnetization expansions above can be further extended with higher-order (multipole) terms, the presented form proved to be sufficient for the description of the major phenomena encountered in the vast majority of electromagnetic materials, both natural and artificial. The general constitutive relations are represented as the linear interrelations between the vector electric and magnetic flux densities and vector electric and magnetic field strengths. The respective proportionality coefficients expressed in the tensor form are usually taken as the extrinsic (phenomenological) material parameters. From relations (2.7), (2.8) and (2.2) we arrive to the constitutive relations of bianisotropic media:

$$\begin{aligned} \mathbf{D} &= \varepsilon_0 \overline{\overline{\varepsilon}} \cdot \mathbf{E} + \sqrt{\varepsilon_0 \mu_0}\, \overline{\overline{\kappa}}_{em}(\omega) \cdot \mathbf{H}, \\ \mathbf{B} &= \mu_0 \overline{\overline{\mu}} \cdot \mathbf{H} + \sqrt{\varepsilon_0 \mu_0}\, \overline{\overline{\kappa}}_{me}(\omega) \cdot \mathbf{E}, \end{aligned} \tag{2.9}$$

where $\overline{\overline{\varepsilon}} = \overline{\overline{1}} + \overline{\overline{\kappa}}_e$, $\overline{\overline{\mu}} = \overline{\overline{1}} + \overline{\overline{\kappa}}_m$ and it is assumed that $\mathbf{P}_0 = \mathbf{M}_0 = 0$. In the case of a simply anisotropic medium $\overline{\overline{\kappa}}_{em} = \overline{\overline{\kappa}}_{me} = 0$. It can be shown (e.g. [5]) that in the lossless medium all the components of tensors $\overline{\overline{\varepsilon}}$ and $\overline{\overline{\mu}}$ are real, whereas $\overline{\overline{\kappa}}_{em}$ and $\overline{\overline{\kappa}}_{em}$ are purely imaginary.

The four tensors involved in the constitutive relations in a general case of bianisotropic medium contain in general 36 complex (nine in each tensor and four tensors) numerical parameters. However, not all these parameters are independent due to the reciprocity conditions (Section 2.5.3) that impose certain conditions on the tensors. Also the lattice symmetry of the material microstructure may restrict certain interactions and thus significantly reduce the number of non-zero and distinctive tensor components. It is noteworthy that magneto-electric coupling may exist in isotropic materials where electric field causes the magnetic response and magnetic field excites the electric polarization, where both these effects are direction independent. Such bi-isotropic materials are characterized by four scalar parameters instead of four tensors. Finally, it is necessary to remark that most metamaterials are described by the general bianisotropy theory, but even the use of so large number of parameters might be insufficient to adequately characterize the properties of many effectively continuous artificial materials.

2.1.4 Piezoelectric materials

Piezoelectricity is an electro-mechanical effect in solids when the electric field is generated in response to the applied mechanical stress. This phenomenon is associated with displacement of positive and negative charges caused by the lattice strain in certain crystals (e.g., quartz, tourmaline) and ceramic materials (e.g. $BaTiO_3$, PZT) with the special crystalline symmetry. The piezoelectric effect is reversible, i.e., voltage applied to the material inflicts the lattice strain and linear deformations of the crystals. Polarization of piezoelectric materials is obtained from the coupled electro-mechanical equations relating stress-strain and stress-charge (direct piezoelectric effect). Since the mechanical stresses and strains themselves are represented by the tensors of the 2nd rank, their relations with electric flux density are generally expressed as the tensors of rank 4. Depending on the crystal class and symmetry of piezoelectric material, the stress-strain and strain-charge tensors contain only a few non-zero components. Nevertheless the constitutive relations for piezoelectrics are much more complicated than for ordinary anisotropic materials because the mechanical stresses and strains themselves are second-order tensors, and hence their relations with electric field and flux density have to be presented by cross-coupling third-order tensors.

On thermodynamic grounds, one can expect that for such materials also the opposite effect exists, which is indeed the case: the application of a potential difference in the material creates a mechanical distortion. This effect is often labeled as the direct piezoelectric effect.

2.1.5 Magnonic materials

Nanostructured magnetic materials can be characterized as effectively continuous media in the long-wavelength limit. Their effective parameters are represented by the Hermi-

tian permeability tensor and the diagonal tensor of permittivity. Owing to the crystalline microstructure of the magnetically active materials, boundaries of the crystal domains and grains create internal magnetic bias which causes resonant precession of the magnetic dipoles in applied high-frequency magnetic fields. The precessing magnetic dipoles in the known ferrimagnetic structures exhibit resonances at GHz frequencies and support spin waves which manifest themselves in very short waves of non-uniform precession travelling through the ensemble of magnetic dipoles. The theoretical analysis of the periodic structures containing ferrimagnetic inclusions in dielectric matrix has shown that the response of such artificial media is determined by the uniform ferrimagnetic resonances of the constituent particles and limited to the GHz frequency range. All the resonant phenomena in such composite materials are described by the Hermitian tensor $\overline{\overline{\mu}}$. In contrast to anisotropic materials with the symmetric tensor $\overline{\overline{\mu}}$, the Hermitian tensor represents a unique notion of gyrotropic medium. The latter feature of magnetically active composite materials is of particular importance for enabling non-reciprocal propagation of both spin and bulk electromagnetic waves. Historically, magnetic nanostructures (called magnonic media) have been associated with excitation of slow spin waves (called magnons) and attempts to increase the frequencies where the spin-wave resonances could be exploited. However, to bring the spin wave phenomena in nanoscaled artificial materials to the THz and optical ranges, it is necessary to resolve the two principal problems of (i) the efficient coupling of electromagnetic fields to non-uniform spin waves and (ii) high losses of spin waves at these frequencies.

2.2 Effectively continuous sheets ("metasurfaces")

If we deal with optically very thin nanostructures (usually impressed into some uniform material layer or located at its surface), the electromagnetic properties of the layer can be formulated in terms of the so-called transition boundary conditions. Consider first an optically thin nanostructured layer consisting of a highly conducting non-magnetic material. The conducting layer of optically small thickness d illuminated by an electromagnetic wave can be presented as an infinitesimally thin induced current sheet. The surface density of the electric current in this sheet is $\mathbf{J} = \tau \mathbf{E}_t$, where $\mathbf{E}_t$ is the surface-averaged tangential component of the total electric field in the layer (the total field is the sum of the incident and reflected ones) and τ is the sheet material parameter called *surface susceptibility*. The electric field $\mathbf{E}$ in the layer can be calculated as the average of electric fields at the layer surfaces $\mathbf{E}(d)$ and $\mathbf{E}(0)$: $\mathbf{E} = [\mathbf{E}(d) + \mathbf{E}(0)]/2$. From the Maxwell equations it follows that the surface current is equal to the jump of the tangential magnetic field across it. Therefore, the equation for the surface current induced in the layer (sheet) can be described through parameter τ in the form of a transition boundary condition:

$$H_t(d) - H_t(0) = \tau[E_t(d) + E_t(0)]/2. \tag{2.10}$$

This condition relates the electric and magnetic fields taken at the two sides of the surface "material". It is invariant with respect to the incidence angle. Together with the known permittivity of the substrate (or that of the host dielectric matrix) (2.10) allows one to find the reflection and transmission coefficients for incident plane electromagnetic waves.

In the case of a thin lossy dielectric layer with complex relative permittivity ε the

parameter τ is related to the bulk permittivity ε as $\tau = \omega\varepsilon_0(\varepsilon-1)d$ [6], and relation (2.10) holds. Similar situation holds in the case when the layer has also magnetic properties. However, in this case the electric field is also discontinuous across the layer and (2.10) should be complemented by relation

$$E_t(d) - E_t(0) = \chi[H_t(d) + H_t(0)]/2. \tag{2.11}$$

For a non-magnetic layer $\chi = 0$. For a magnetic one it is related to the bulk permeability as $\chi = \omega\mu_0(\mu - 1)d$. For anisotropic magneto-dielectric media parameters ε and μ are tensors, and therefore in the general case τ and χ can be tensors, too.

The description of a natural surface material in terms of surface material parameters τ and χ is equivalent to its description in terms of bulk material parameters ε and μ. The last ones result in the same solution of any boundary electromagnetic problem if the layer finite thickness d is small and it is properly taken into account. However, this equivalence holds only because for a natural magneto-dielectric layer there are very many atoms across the layer and the material is anyway inherently bulk. Its representation as an effective surface is an additional approximation which simplifies the solution of the boundary problems.

For nanostructured surface materials, say, for a grid of nanoparticles located on a substrate or embedded into a dielectric matrix the presentation in terms of the continuous sheet can be called "surface homogenization". Such structures were called metasurfaces or metafilms in [1, 2]. Bulk material parameters ε and μ cannot be introduced for a metasurface for a number of reasons. Deficiency of the bulk parameter description in this case can be illustrated considering beam propagation across the layer (oblique incidence). In a bulk material layer, the phenomenon of the wave refraction is observed, which leads to a lateral shift of the propagating beam behind the layer. However, a monolayer of small scatterers does not refract the incident wave, and no beam shift is possible. Instead, induced electric dipoles of the metasurface cause a jump of the magnetic field given by equation (2.10), and magnetic dipoles results in a jump of the electric field given by equation (2.11). Thus, nanostructured surface materials can be electromagnetically characterized by surface material parameters τ and χ (tensorial in the general case) but cannot be described by bulk material parameters.

2.3 Photonic crystals

During the last few decades much attention has been attracted to electrodynamic properties of periodical structures where permittivity and/or permeability are periodical functions of the coordinates. Following quantum mechanics such structure are referred to as "photonic crystals" (PC) or "band-gap structures". There is an analogy between Maxwell's equations for electromagnetic wave propagation and Schrödinger's equation for electron propagation in a periodic potential. Consider a monochromatic electromagnetic wave of frequency ω propagating in a medium whose permittivity varies from point to point in space, satisfying the periodicity condition $\varepsilon(\mathbf{r}) = \varepsilon(\mathbf{r} + \mathbf{a})$. We can write $\varepsilon(\mathbf{r}) = \varepsilon_{\text{av.}} + \Delta\varepsilon(\mathbf{r})$, where the average value of $\Delta\varepsilon(\mathbf{r})$ over the lattice period is zero. The last term (more exactly $k^2\Delta\varepsilon$, where k is the wave number in the medium of permittivity $\varepsilon_{\text{av.}}$) plays the role of the scattering potential in Schrödinger's equation.

An electron in a semiconductor crystal (periodic arrangement of atomic potentials) and a photon in a PC (periodically modulated dielectric or magneto-dielectric medium) possess a variety of band gaps, where the propagation is forbidden for certain ranges of wavelengths. Using different materials (different dielectric constants) and by adjusting geometrical parameters, the propagation of light can be modified in a controllable manner.

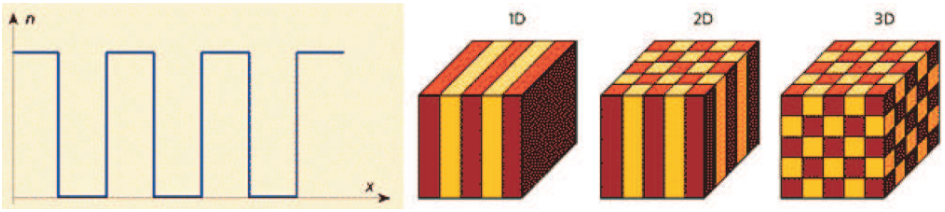

Figure 2.1: Left – The coordinate dependence of the local refraction index n (n is the square root of permittivity $\varepsilon(\mathbf{r})$) in photonic crystals shown in the right panel. Right panel – the schemes of typical 1D, 2D and 3D photonic crystals.

Band gaps (BG) appear due to the so-called Bragg reflection. The condition of this reflection is an integer number of half wavelengthes equal to the the lattice period along the propagation direction. Within a band gap the light is reflected from the crystal planes in phase and as a result totally reflects from the surface of a PC. In an infinite crystal such a wave cannot propagate, in other words, its wave number is imaginary and it should exponentially decay if it is excited by any source. For finite-thickness PC the BG are important if the thickness is larger than the decay distance D. The last one is related to the BG frequency width $\Delta\omega$, lattice period a and the operating frequency ω as [3]:

$$D = \frac{a\omega}{\pi\Delta\omega}. \tag{2.12}$$

For a harmonically varying permittivity $\Delta\varepsilon(z) = A\cos\Omega z = A\cos(2\pi z/a)$ one has [3]:

$$\Delta\omega = \omega\frac{A}{\varepsilon_{\text{av.}}}. \tag{2.13}$$

An important feature of PC is that the propagating eigenwaves in them are so-called Bloch waves. A Bloch wave is a product of the factor describing a propagating plane wave with wave number q, i.e. $\exp(-jqz)$, and a certain function $u(\mathbf{r})$ which is periodic with the lattice period a. In the case when the wave propagates not along the lattice coordinate axis, the plane wave is described as $\exp(-j\mathbf{q}\cdot\mathbf{r})$ and $u(\mathbf{r})$ is periodic with a vector period $\mathbf{a}(\mathbf{a}_x, \mathbf{a}_y, \mathbf{a}_z)$. The wave vector $\mathbf{q}$ in periodical media is called the Bloch wave vector.

To understand the properties of PC and their difference from natural materials it is convenient to employ the so-called isofrequency surfaces (or their sections by a coordinate plane called isofrequency contours). Isofrequency surfaces were introduced in the beginning of the XIX century by Fresnel and have been since that time widely used in optics of anisotropic materials. An isofrequency surface is a locus of the ends of wave vectors (the Bloch wave vectors in the case of PC) at a fixed frequency. The isofrequency surface has a periodic pattern. In Fig. 2.1 besides a 1D PC (periodical stack) the so-called chess-board PC are shown as examples of 2D and 3D PC. Isofrequency contours of a 3D chess-board PC depicted in Fig. 2.1, right panel, are shown in Fig. 2.2 for three different frequencies.

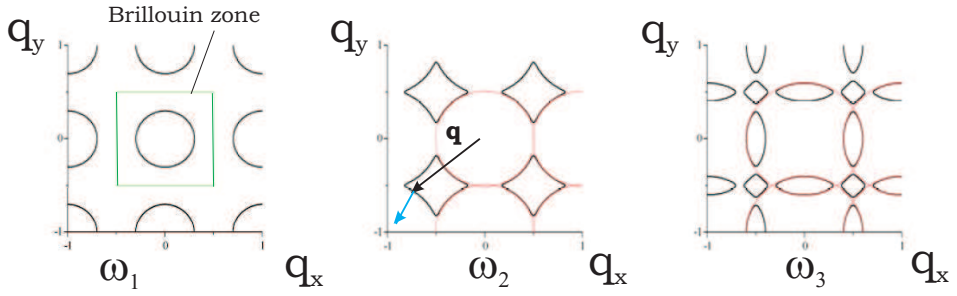

Figure 2.2: Typical isofrequency contours for a PC of at three different frequencies above the first BG.

Two frequencies refer to the 2nd pass-band (laying above the lowest BG), and the third one refers to the 3rd pass-band (above the 2nd BG). The group velocity of the eigenwave is directed along the normal to the isofrequency surface and points to the direction of the isofrequency shift with the frequency increase. It is shown as a blue arrow in Fig. 2.2.

The PC for which these isofrequencies have been calculated is geometrically isotropic. For continuous isotropic media all isofrequency contours are obviously circular [4], but the PC is not a continuous medium. We can see that isofrequency contours of PC deviate from circular ones very strongly. This difference is the manifestation of the general phenomenon called strong spatial dispersion. In this situation the dispersion of signals in PC is very different from that in continuous media. Other manifestations of strong spatial dispersion are band gaps (Bragg reflection of waves whose frequencies belong to band gaps) and the existence of multiple scattered plane waves.

In PC one observes many other interesting and useful phenomena such as all-angle negative refraction, which leads to the parallel-plate focusing almost without aberrations, extraordinary dispersion (so-called photonic super-prism is a class of optical components based on this effect), modes concentration in cavities, defect waveguiding, surface states, non-linear effects such as modification of radiation spectra of quantum emitters and many others. Most of these effects are tightly related to the strong spatial dispersion in these structures. Strong spatial dispersion in PC occurs at frequencies above the lower edge of the first low-frequency band gap. This frequency is called the lowest Bragg frequency or frequency of the first spatial resonance of the lattice. At lower frequencies band-gap structures behave nearly as continuous media with uniform permittivity $\varepsilon(\mathbf{r}) = \varepsilon_{\text{av}}$. Therefore at so low frequencies artificial lattices are not called PC and are referred to as artificial dielectrics. If their constitutive elements are magnetic, they are called composite magnetics. An exception is the class of metamaterials which are as a rule also lattices operating at frequencies below the first spatial resonance. Due to the resonance response of their inclusions metamaterials cannot be considered as media whose permittivity is averaged over the total volume of the unit cell. This makes their electromagnetic characterization so problematic.

Effective material parameters ε and μ can be formally introduced for PC also at high frequencies above the first band gap using definitions (2.2) and (2.5). However, as it is known for media with strong spatial dispersion [4], these material parameters (though they can be used for studying the eigenwaves in the unbounded lattices) become useless for solving boundary problems. Therefore they cannot be used as characteristic material

parameters. There is little physical meaning in these parameters since in the photonic crystal regime the electric response of the lattice unit cell to the propagating electromagnetic wave cannot be separated from the magnetic response. The wave interaction with any unit cell is fully dynamic. Therefore permittivity and permeability of the discrete medium in formulas (2.5) above the first band gap of a PC are functions of the wave vector $\mathbf{q}$.

In the case of two-dimensional structures ("metasurfaces", see Section 2.2), the analogy of photonic crystals is the diffraction grating, where the separations between particles forming a two-dimensional lattice are comparable with the wavelength. Also in this case the description in terms of homogenized sheets of polarization looses its physical meaning.

2.4 Electromagnetic classification of nanostructured materials

The possibilities of combining nanosized inclusions are infinite and the possibilities for the realized effective material behaviour of are vast. From the point of view of electromagnetic properties, most interesting are "metamaterials", generically defined as arrangements of artificial structural elements, designed to achieve advantageous and unusual electromagnetic properties.

Inspecting different types of existing nanostructured materials (NSM) (and prospective nanostructured materials which are under discussion in the current literature) we can find many types of them which satisfy the above definition of metamaterial (MTM). To show the place of nanostructured MTM among all nanostructured materials it is instructive to introduce a classification of NSM. Possible classification is presented in form of a table and is related to the characterization of linear electromagnetic properties of NSM. Different types of NSM should be described by different sets of electromagnetic parameters. This classification takes into account the internal geometry of NSM and most important linear electromagnetic properties of constituents and effective medium formed by them. The left upper cell has rich content which is detailed in Table 2.1. The most important criterion of the classification is the dimension of the array of constituents which forms the nanostructured material. 3D or bulk materials correspond to structures with a large number of constitutive elements in the array along any direction. 2D or surface materials correspond to the case when the artificial material is a layer including only 1-3 constitutive elements across it. Analogous classification can be possibly suggested for non-electromagnetic MTM.

MTM of the surface type were called metasurfaces in [12, 13] and metafilms in papers [1, 2]. Notice that in these papers a consistent method of electromagnetic characterization of metasurfaces (metafilms) comprising one inclusion across the layer thickness was suggested. Linear (directional) structures with nanosized inclusions are optical waveguides with nanoinclusions, plasmonic and polaritonic nanochains. They are called in this table metawaveguides, but are not referred to as "materials" since the concept of material is usually not applied to 1D structures.

The second criterion of the classification is the optical size of the unit cell in the visible and near-IR frequency range where the known nanostructures usually operate (i.e.

Table 2.1: Nanostructures classified by their linear electromagnetic properties (q is the effective wave number in the structure and a is the size of the lattice unit cell.)

Nanostructures (NS)	Optically dense $(qa) < 1$	Optically sparse $(qa) > 1$	Dense in one direction, in other direction(s) either sparse or with extended inclusions
3D bulk materials	Bulk MTM with small inclusions, bulk NSM without MTM properties	Photonic crystals, quasi-crystals, sparse random composites	Wire media, multilayer plasmonic structures (fishnets, solid metal-dielectric nanolayers)
2D, sheet materials	Metasurfaces (metafilms), nanostructured sheets without MTM properties	Plasmonic diffraction grids, optical bandgap and frequency selective surfaces	Artificial nanostructured surfaces with long inclusions or slots
1D, lines	Metawaveguides	Not yet known but possible	Impossible

possess useful and unusual electromagnetic properties). Large optical size practically implies $|q|a > 1$. In this range the structure cannot be characterized by local material parameters (neither bulk nor surface ones). In the opposite case $|q|a \ll 1$ the structure in principle can be characterized by local parameters and can be referred to as MTM. The same structure at different frequencies can be referred either to optically dense or to optically sparse types.

The third criterion is the presence or absence of properties which allow us to refer or not to refer an optically dense material to MTM. Usually though not always these useful unusual properties are enabled by resonances of inclusions.

Let us give some comments on Table 2.1. Nanostructured composites can be designed for whatever purpose and not always possess any interesting or unusual electromagnetic properties. Instead they can possess useful thermal and mechanical properties, for example, or they can have specially engineered electric conductivity. The combinations of these properties are used for example in thermoelectric elements. Such materials are not referred to MTM in this table. Optically sparse nanostructures (photonic crystals) are not referred to MTM since they do not fit the concept of effectively continuous materials.

Optically dense surface nanostructures are, for example, plasmonic island nanofilms and chemically roughened metal surfaces. The constituents are metal islands or random nanocorrugations. They are used mainly in sensing applications: molecular clusters and even separate molecules utilizing the so-called surface-enhanced Raman scattering (SERS) scheme. This scheme is based on the effect of the local field enhancement in the vicinity of such a surface. The property of plasmon resonance which is responsible for this effect is definitely useful, however, it is rather usual from the electromagnetics point of view. Extensive literature has been devoted to such structures since the discovery of SERS in the 1970s. On random plasmonic surfaces the local field enhancement is the same as for a single plasmonic nanoparticle and is observed only at points on top of the particle (or at the edges of a nanoisland). Plasmon resonance in metal particles has been known

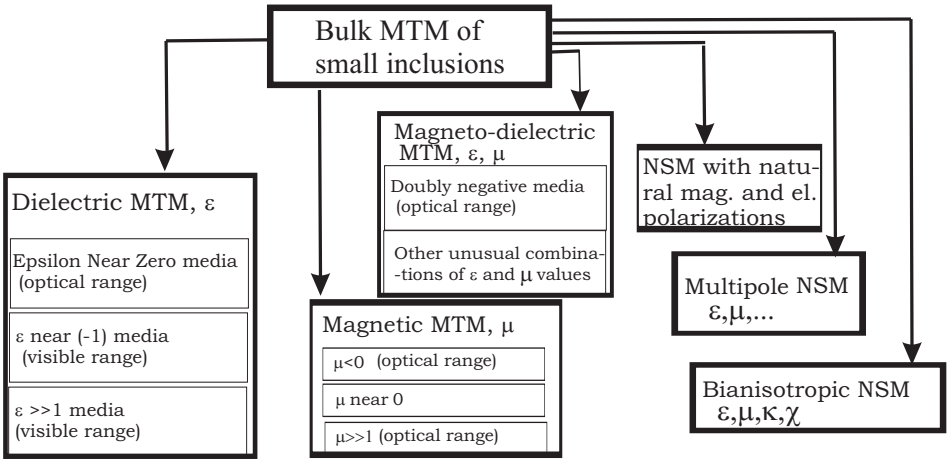

Figure 2.3: Classification of bulk nanostructured MTM of small inclusions. Optical range in this diagram by definition covers infrared, visible and near ultraviolet ranges.

for a long time. Therefore we do not refer these structures to MTM. However, if the nanostructured plasmonic surface is regular, it possesses an unusual property: the strong enhancement of the averaged field in such structures. Such artificial surfaces probably refer to metasurfaces. Nanostructured surfaces of vertical (aligned) metal nanorods grown on the metal substrate at the plasmon resonance of the rods enhance the field at the plane corresponding to the upper edges of the rods [14]. Such structures should be also referred to metasurfaces. In general, nanostructured metasurfaces are self-resonant grids possessing certain regularity either in the arrangement of resonant elements or in their orientation. Such grids can comprise separate plasmonic scatterers on a dielectric substrate or plasmonic corrugations. They also can be performed as solid metal screens of nanometer thickness with slots or holes. For example, metal nanolayers with subwavelength slots support surface plasmon polariton waves whose dispersion is determined by these slots (see e.g. in Chapters 25 and 26 of [13]). Another important example of a metasurface is a monolayer optical fishnet (see e.g. in Chapter 29 of [13]). This monolayer is formed by a pair of parallel silver or gold periodically slotted nanolayers with nanogap between them. The slots in fishnet structures are non-circular and are rather optically large.

Abundant literature is devoted to nanostructured waveguides (metawaveguides in our classification). Their useful and unusual property is the subwavelength channel for the guided wave observed in plasmonic nanochains (see e.g. in [15]) and nanostructured fibers with plasmonic insertions (see e.g. in [16]). They also can be used for frequency filtering of optical signals on the nanoscale level (e.g. in [17]).

Multilayer optical fishnets and multilayer metal-dielectric nanostructures (see e.g. [18]–[23]) are important types of MTM. Multilayer optical fishnets demonstrate not only the negative phase shift of the wave across the structure (i.e. backward wave propagation), the negative group velocity has been observed as well (i.e., the inverse direction of the pulse peak velocity with respect to the energy transport direction). In multilayer nanostructures of alternating continuous metal and dielectric nanolayers one experimentally demonstrated the subwavelength optical imaging in the far zone of the optical object (e.g. [24]). Note that known fishnets do not offer subwavelength imaging in the backward-wave frequency

range, so none of them can make a Pendry perfect lens. These structures are referred to MTM in our table since the thickness of their layers is much smaller than the wavelength. However, they possess strong spatial dispersion for waves propagating obliquely to the structure or along it because the constituents are extended and the tangential periods (in fishnet structures) are electrically large.

For another type of such MTM – wire media – the effect of spatial dispersion is crucial for their unusual properties (see e.g. in Chapter 15 of [12]). Wire media in the optical range are optically dense arrays of optically long metal nanowires or carbon nanotubes. Wire media can be grown on a substrate or prepared by embedding nanowires into porous glass or porous plastic fiber matrix. If nanowires are grown on a substrate, they can be optically short and then refer to metasurfaces (see Section 2.2). Arrays of aligned nanorods and nanotubes should be referred to nanowire media if the optical length of cylinders is enough. Nanostructured wire media are spatially dispersive in the infrared range [24]. In the visible range optically dense lattices of parallel metal nanowires become a uniaxial dielectric medium without strong spatial dispersion [25].

In Fig. 2.3 bulk MTM are classified based on their material parameters. Optically dense nanocomposites can be artificial dielectric media with unusual permittivity, i.e. ε close to 0 or to (-1) or very high ($\varepsilon > 10$ in the visible range where usual materials (except some very lossy semiconductors and liquid crystals) have rather low permittivity ($\varepsilon < 6 \dots 7$). Artificial magnetic media, possessing negative permeability in the optical range are also MTM. Not only media with negative μ deserve to be referred to MTM, media with $\mu \approx 0$ or even $\mu = 2$ in the optical range are also MTM. Media with both negative permittivity and permeability represent the most known type of MTM, however if $\varepsilon = 0$ and $\mu = 2$ in the visible range such material should be also referred to magneto-dielectric MTM. Optically dense nanocomposites with plasmonic inclusions refer to MTM for both cases of regular and random arrangements. Random nanocomposites possess additional scattering losses whereas regular plasmonic composites do not. Therefore regular plasmonic composites are more promising for applications. They can also behave as resonant multipole media and resonant bianisotriopic media formed by nanoparticles. In both these cases the number of material parameters describing such media is larger than two. The difference between magneto-dielectric nanostructured media, multipole and bianisotropic media is discussed in Chapter 2 of [12].

The consistent classification of nanostructured MTM is helpful to avoid the most dangerous pitfalls in their electromagnetic characterization: the inconsistent classification of the material under study. In many publications describing metasurfaces, i.e. MTM layers with only 1-2 resonant inclusions over the layer thickness, authors of [18]– [20], [26]– [34] and other similar works treat these metasurfaces as bulk media. Multipole and bianisotropic bulk media were described as simple magneto-dielectrics (characterized by ε and μ), for example, in works [35]– [47].

2.5 Some important concepts of complex-media electromagnetics and optics

2.5.1 Resonant and non-resonant materials

In some frequency regions the permittivity and permeability of materials can exhibit resonances, where these parameters abruptly vary with the frequency of applied fields. For resonant structures their permittivity and permeability (if the last one is also resonant) suffer large losses within the resonant band. For non-resonant structures permittivity and permeability change slowly when the frequency is varied, and usually have much smaller losses. Whilst the name might suggest otherwise, non-resonant composite materials do have frequencies at which their particles (for composite media – inclusions) are resonant, but these resonances occur at higher frequencies. Conversely to resonant nanostructures, non-resonant ones have a broad bandwidth at which their relative permittivity can make a strong contrast to the free space (significantly different from unity). In the optical range these materials are metals and semiconductors. This broadband contrast is their primary advantage in design of various devices. Their main disadvantage is that they have small dynamic range of material parameters. Provided they do not have negative permittivity or very large positive one, simple-shape particles such as spheres or ellipsoids are non-resonant. In the case of metamaterials, the resonant frequencies strongly depend on the shape and the size of inclusions, in addition to their chemical composition.

2.5.2 Quasi-static limit

In the quasi-static limit the optical size of the medium unit cell is by definition at least 100 times smaller than the wavelength in the medium. In this case the phase variation of the local field over the unit cell is negligible even for complex-shaped particles, and the phenomena of artificial magnetism and bianisotropy in reciprocal media disappear. This situation corresponds to most natural media in the optical frequency range (even more so in the radio frequency range). Artificial magnetism is never observed in natural media, only bianisotropy is not negligible for some natural materials in the visible frequency range (optical chiral materials, like sugar solution in water, for example).

For composite materials of non-magnetic inclusions in the quasi-static limit only the permittivity remains different from that of the host medium. If inclusions are magnetic (for nanostructured materials this corresponds to arrays of nanomagnets), the permeability in the quasi-static limit can be different from unity. In the literature one can meet opinions that the correct electromagnetic characterization of materials in the condensed form of a few material parameters is possible only in the quasi-static limit when the frequency dispersion of the medium response is absent (see e.g. [7–11]). Following to these authors we should have recognized the concept of artificial magnetism and bianisotropy as incorrect ones. However, if the medium satisfies the locality limitations, the basic theory does not inhibit the electromagnetic characterization of the medium in terms of permittivity, permeability and magnetoelectric coupling tensors. The only fundamental limitation to the electromagnetic characterization of composite media in condensed form is, in our opinion, the locality limitation (see more detailed discussion is Section 2.5.5).

2.5.3 Reciprocity and non-reciprocity

The principle of reciprocity is fundamental for the electromagnetic media, and all electromagnetic materials can be cast in the two categories: reciprocal and non-reciprocal media. The notion of reciprocity is directly related to the symmetry with respect to the time inversion operation. Most natural materials are reciprocal, except for naturally biased magnetic materials, such as hard ferrites and antiferromagnetics, and externally biased media, e.g. magnetized plasma, voltage biased semiconductors, etc. In practical terms, reciprocity means an invariance of the media response when the positions of the field source and probe are interchanged. For bianisotropic medium to be reciprocal, its constitutive parameters must obey the following relations (e.g., [5]):

$$\overline{\overline{\varepsilon}} = \overline{\overline{\varepsilon}}^T, \qquad \overline{\overline{\mu}} = \overline{\overline{\mu}}^T, \qquad \overline{\overline{\kappa}}_{me} = -\overline{\overline{\kappa}}_{em}^T \equiv j\,\overline{\overline{\kappa}}, \tag{2.14}$$

where superscript T denotes the transpose operation. The tensor $\overline{\overline{\kappa}}$ (real for lossless media) is usually called the *chirality tensor*. From these relations we see that the permittivity and permeability of reciprocal media are symmetric tensors, whereas the tensors of magnetoelectric cross-coupling are negatively transposed. It is noteworthy that the reciprocity conditions above reduce the number of the parameters describing bianisotropic medium from 36 to 21 complex valued quantities.

In the general case of non-reciprocal bianisotropic medium the constitutive relations take the form

$$\mathbf{D} = \varepsilon_0\,\overline{\overline{\varepsilon}} \cdot \mathbf{E} + \sqrt{\varepsilon_0\mu_0}\,(\overline{\overline{\chi}} - j\overline{\overline{\kappa}}) \cdot \mathbf{H}, \tag{2.15}$$

$$\mathbf{B} = \mu_0\overline{\overline{\mu}} \cdot \mathbf{H} + \sqrt{\varepsilon_0\mu_0}\,(\overline{\overline{\chi}} + j\overline{\overline{\kappa}})^T \cdot \mathbf{E}. \tag{2.16}$$

Permittivity and permeability of general non-reciprocal media contain antisymmetric parts: they are Hermitian tensors with complex conjugated off-diagonal elements. The additional magnetoelectric tensor $\overline{\overline{\chi}}$ describes the non-reciprocal field coupling effect and is called *Tellegen's tensor*. The anti-symmetric parts of permittivity and permeability as well as the Tellegen tensor are non-zero only if there is an external field which changes sign (breaks the symmetry) under the time-reversal operation. This stimulus can be an external magnetic bias field or internal magnetization of the medium.

All bianisotropic materials can be categorized into 14 classes based upon 7 reciprocal and 7 non-reciprocal components of their material parameter tensors which are related to the reciprocal or non-reciprocal nature of their constituents [5].

2.5.4 Spatial dispersion

Spatial dispersion is the name of an effect based on non-locality of electromagnetic response in materials. It expresses that material polarisation at a certain point in space is influenced by electric fields at neighbouring points. Spatial dispersion is one of the key notions in the theory of artificial electromagnetic materials and the first order spatial dispersion results in chirality, while the second order dispersion results in artificial magnetism. Following [5], we will next briefly describe approaches to effective material parameter modelling of weak spatial dispersion and explain how spatial dispersion determines chirality and artificial magnetism in metamaterials.

To describe a metamaterials with its nanoinclusions, we need the microscopic Maxwell equations. Finally, we are however only interested in the macroscopic (material) properties of the metamaterials. The macroscopic Maxwell equations (1.2) follow from volume averaging of the microscopic Maxwell equations, and this averaging can only be done easily if the material is weakly spatially dispersive. On this route, it is important to distinguish weak spatial dispersion from strong spatial dispersion. Weak spatial dispersion is when the polarisation current at a certain point of the medium is influenced only by what happens at neighbouring points inside the same unit cell of the medium (in practice inside one particle). Strong spatial dispersion is when phenomena at a certain point of the medium are also influenced by what happens outside the unit cell, that is by (many) neighboring unit cells. Averaging "smoothes" the current and charge distributions and the actual microscopic fields, determined by movements of individual electrons, are replaced by averaged charge and current densities, which are uniform over one unit cell of the structure.

Direct averaging of microscopic field equations in source-free regions results in

$$\nabla \times \mathbf{E} = -j\omega\mathbf{B}, \qquad \frac{1}{\mu_0}\nabla \times \mathbf{B} = j\omega\varepsilon_0\mathbf{E} + \mathbf{J}^{\text{ind}}$$

$$\varepsilon_0\nabla \cdot \mathbf{E} = \rho^{\text{ind}}, \qquad \nabla \cdot \mathbf{B} = 0. \tag{2.17}$$

Here the field vectors are the averaged (over a physically small volume) microscopic electric and magnetic fields, and $\mathbf{J}^{\text{ind}}$ and ρ^{ind} are the volume-averaged microscopic current density and charge density. If we formally define induction vectors as

$$\mathbf{D} = \varepsilon_0\mathbf{E} + \frac{\mathbf{J}^{\text{ind}}}{j\omega}, \qquad \mathbf{H} = \mu_0^{-1}\mathbf{B}, \tag{2.18}$$

the macroscopic Maxwell equations take the familiar form:

$$\nabla \times \mathbf{E} = -j\omega\mathbf{B}, \qquad \nabla \times \mathbf{H} = j\omega\mathbf{D}$$

$$\nabla \cdot \mathbf{D} = 0, \qquad \nabla \cdot \mathbf{B} = 0. \tag{2.19}$$

Polarization is induced by electric fields in the medium, so in the most general case of nonlocal (spatially dispersive) linear reciprocal media we can write for the induced current $\mathbf{J}^{\text{ind}} = \mathbf{J}$ the relation

$$\mathbf{J}^{\text{ind}}(\mathbf{r}) = \int_V \overline{\overline{K}}(\mathbf{r}, \mathbf{r}') \cdot \mathbf{E}(\mathbf{r}')\, dV', \tag{2.20}$$

where V is the sample volume.

In principle, the kernel dyadic $\overline{\overline{K}}(\mathbf{r}, \mathbf{r}')$ can be measured or theoretically modelled, and then (2.20) can be used as a *constitutive relation* together with $\mathbf{H} = \mathbf{B}/\mu_0$. Clearly, this formalism which involves solving a system of integro-differential equations is not really practical. If the spatial dispersion is *weak*, that is, the polarization in a given point depends only on the values of the electric field in a near neighbourhood, we can simplify the model replacing the integral relation (2.20) by a relation which includes only low-order spatial derivatives of the field. For isotropic materials, this expansion can be conveniently written in terms of the differential operator ∇:

$$\mathbf{J}^{\text{ind}}(\mathbf{r}) = j\omega\left[\alpha_0\mathbf{E}(\mathbf{r}) + \alpha\nabla \times \mathbf{E}(\mathbf{r}) + \beta\nabla\nabla \cdot \mathbf{E}(\mathbf{r}) + \gamma\nabla \times \nabla \times \mathbf{E}(\mathbf{r})\right]. \tag{2.21}$$

Here we have kept only the derivatives up to the second order. Substituting into (2.18), we get the constitutive relations in form

$$\mathbf{D} = \varepsilon\mathbf{E} + \alpha\nabla\times\mathbf{E}(\mathbf{r}) + \beta\nabla\nabla\cdot\mathbf{E}(\mathbf{r}) + \gamma\nabla\times\nabla\times\mathbf{E}(\mathbf{r}), \qquad \mathbf{H} = \mu_0^{-1}\mathbf{B}. \tag{2.22}$$

The induction fields can be re-defined [5] in order to write these relations in a simpler form:

$$\mathbf{D} = \varepsilon\mathbf{E} - j\omega\frac{\alpha}{2}\mathbf{B} + \beta\nabla\nabla\cdot\mathbf{E}, \qquad \mathbf{H} = \mu^{-1}\mathbf{B} - j\omega\frac{\alpha}{2}\mathbf{E}, \tag{2.23}$$

where

$$\mu = \frac{\mu_0}{1-\omega^2\mu_0\gamma}. \tag{2.24}$$

Comparing with the material relations of chiral media (2.9), we see that the effect of reciprocal magneto-electric coupling (chirality) is a non-local effect of the first order, because the coupling term is proportional to the coefficient α in the Taylor expansion (2.21). Likewise, the artificial magnetism (permeability μ different from unity) is a non-local effect of the second order, defined by the expansion coefficient γ in (2.21).

When the inclusions forming a composite material as well as the distances between them are very small (in terms of the wavelength), the spatial dispersion is negligible, and the composites behave as "usual materials". If the inhomogeneity scale is of the order of the wavelength or larger, this is a photonic crystal (Section 2.3), and it cannot be described by effective material parameters. If we want to realize some unusual and novel material parameter values, we have to work in the "gray zone" between these two regimes: The inhomogeneities should be not too small, in order to have pronounced artificial magnetism and other interesting metamaterial properties, but also not too large, in order to allow for effective medium description. This defines the limits of the validity regions of homogeneous models and makes the electromagnetic characterization difficult. As just one of the complication examples, note that the second-order model (2.23) contains also the explicit second-order derivative terms, proportional to the coefficient β. That term is usually neglected in models of artificial magnetic materials. In some cases this is justified, but in many situations this leads to non-physical behaviour of the "effective" permeability [48].

2.5.5 Locality requirements in description of effectively homogeneous materials

If all the material parameters depend only on the frequency and possibly on the spatial coordinates (assuming slow variations without abrupt changes) but are invariant to the direction into which the applied field is changing in space (direction of the wave propagation, in the case of plane-wave excitation), one tells that the medium is *local*. In other words, for local media the susceptibilities entering (2.7) and (2.8) depend only on the material properties (including the material frequency dispersion) and do not depend on the position of external sources, provided they create the same applied field at the observation point.

For effectively continuous media the locality requirements are fulfilled [4], and, on the other hand, they cannot be fulfilled. for band-gap structures. For isotropic magneto-dielectric media the locality implies (see e.g. in [4]) the system of following conditions:

- Passivity (for the temporal dependence $e^{-i\omega t}$ it implies $\mathrm{Im}(\varepsilon) > 0$ and $\mathrm{Im}(\mu) > 0$ simultaneously at all frequencies, for $e^{j\omega t}$ the sign of both $\mathrm{Im}(\varepsilon)$ and $\mathrm{Im}(\mu)$ should be negative). The violation of passivity in the energetically inactive media (without any electromagnetic field sources at frequency ω) means the violation of the 2nd law of thermodynamics;

- Causality (for media with negligible losses it corresponds to the conditions $\partial(\omega\varepsilon)/\partial\omega > 1$ and $\partial(\omega\mu)/\partial\omega > 1$. This also means that in the frequency regions where losses are negligibly small, the material parameters obviously grow versus frequency: $\partial(\mathrm{Re}(\varepsilon))/\partial\omega > 0$ and $\partial(\mathrm{Re}(\mu))/\partial\omega > 0$;

These mandatory properties of effectively continuous media follow from the independence of the material parameters from the wave vector $\mathbf{q}$ (for a given frequency this means the independence of electromagnetic parameters (EMP) on the propagation direction) [4]. For anisotropic reciprocal media similar requirements of locality can be formulated for all components of tensor material parameters if they are written in a suitable system of coordinates where these tensors are diagonal. It is more difficult but also possible to formulate the locality limitations for bianisotropic and non-reciprocal media.

It is worth noticing that the local bianisotropic constitutive relations model not only local dielectric response, but also effects of chirality and artificial magnetism which are physically non-local effects [4]. In fact, chirality and artificial magnetism are manifestations of the so-called weak spatial dispersion which allows the condensed description of some slightly non-local media in terms of local material parameters by the cost of introducing two additional material parameters (permeability and chirality tensors) [5] (see more in Section 2.5.4). In the framework of the weak spatial dispersion models, the locality requirement assumes that the spatial dispersion is so weak that the constituent particles of the composite medium interact only through their near fields. The wave interaction between particles is not important. Only particles inside a rather optically small volume around the reference particle effectively influence to the local field acting to the reference particle. This volume is often called the Lorentz sphere, though for many possible array geometries it is not a spherical region. The contribution of particles beyond the Lorentz sphere (i.e. located practically in the far zone of the reference particle) is not so important for the response of the reference particle. In other words, the polarization response of the medium calculated at a reference point is local because it is determined by the polarization within the Lorentz sphere. This sphere is an optically small volume around the reference point and the phase of the wave over this volume is effectively uniform. This is the meaning of the term locality. It is clear why for effectively discrete media the locality does not hold. Particles adjacent to the reference one in the effectively discrete media are located in its far zone, and the Lorentz sphere cannot be introduced.

It is interesting to note that in the case of the bianisotropy and artificial magnetism we cannot neglect the spatial variations of the field acting to the reference particle. These effects appear namely due to the small spatial variation of the local field. However, the concept of the Lorentz sphere (over which the phase shift of the wave is negligible) is qualitatively applicable for bianisotropic media and for artificial magnetics. There is no contradiction in the model because the bianisotropy and artificial magnetism appear only when optically small particles have a complex internal geometry, and therefore they feel even a very small spatial variation of the local field.

The two locality requirements are complemented by the requirement on absence of radiation losses in optically dense arrays with uniform concentration of particles [5]. Such arrays do not scatter the incident wave, they only refract it. If particles of the arrays are lossless, i.e. their material parameters are real, there is no dissipation in particles and no radiation losses in the array. Then the refracted wave must propagate without attenuation. This means that the effective material parameters of lossless materials with regular internal structure should take real values.

Bibliography

[1] E.F. Kuester, M.A. Mohamed, M. Piket-May, C.L. Holloway, Averaged transition conditions for electromagnetic fields at a metafilm, *IEEE Trans. Antennas Propag.* **51** (2003) 2641

[2] C.L. Holloway, A. Dienstfrey, E.F. Kuester, J.F. O'Hara, A.A. Azad, A.J. Taylor, A discussion on the interpretation and characterization of meta-films/metasurfaces: The two-dimensional equivalent of metamaterials, *Metamaterials* **3** (2009) 100

[3] K. Sakoda, *Optical properties of photonic crystals*, Springer: Berlin-Heidelberg-new Yors, 2005.

[4] L.D. Landau and E.M. Lifshitz, *Electrodynamics of continuous media*, Pergamon Press, Oxford, 1960.

[5] A.N. Serdyukov, I.V. Semchenko, S.A. Tretyakov, A. Sihvola, *Electromagnetics of bi-anisotropic materials: Theory and applications*, Amsterdam: Gordon and Breach Publishers, 2003.

[6] Sergei Tretyakov, *Analytical Modeling in Applied Electromagnetics,* Norwood, MA: Artech House, 2003.

[7] B. Hallouet, B.Wetze, R. Pelster, *Journal of Nanomaterials* **2007** (2007) article ID 34527.

[8] H. Leinders, A. Enders, *Journal de Physique I* **5** (1995) 555.

[9] C. Brosseau, A. Beroual, *The European Physical JournalApplied Physics* **6** (1999) 23.

[10] F. Wu, K. W. Whites, *IEEE Transactions on Antennas and Propagations*, **49** (2001) 1174.

[11] D. J. Bergman, *Physics Reports* **43** (1978) 377.

[12] *Metamaterials Handook. Volume 1. Theory and phenomena of metamaterials,* F. Capolino, Editor, Boca Raton-London-New York: CRC Press, 2009.

[13] *Metamaterials Handook. Volume 2. Applications of metamaterials,* F. Capolino, Editor, Boca Raton-London-New York: CRC Press, 2009.

[14] Q. Xu, J. Bao, F. Capasso, G.M. Whitesides, Surface plasmon resonances of free-standing gold nanowires fabricated by nanoskiving, *Angew. Chem.* **45** (2006) 3631

[15] A. Alu, N. Engheta, Guided propagation along quadrupolar chains of plasmonic nanoparticles, *Physical Review B* **79** (2009) 235412

[16] J. Elser, A.A. Govyadinov, I. Avrutsky, I. Salakhutdinov, V.A. Podolskiy, Plasmonic Nanolayer Composites: Coupled Plasmon Polaritons, Effective-Medium Response, and Sub-diffraction Light Manipulation, *Journal of Nanomaterials* (2007) paper ID 79469 (1-8)

[17] N. Engheta, Circuits with light at nanoscales: Optical nanocircuits inspired by metamaterials, *Science* **317** (2007) 1698

[18] G. Dolling, C. Enkrich, M. Wegener, C.M. Soukoulis, S. Linden, Low-loss negative-index metamaterial at telecommunication wavelengths, *Science* **312** (2006) 892

[19] T.F. Gundogdu, N. Katsarakis, M. Kafesaki, R.S. Penciu, G. Konstantinidis, A. Kostopoulos, E.N. Economou, and C.M. Soukoulis, Negative index short-slab pair and continuous wires metamaterials in the far infrared regime, *Opt. Express* **16** (2008) 9173

[20] M. Kafesaki, I. Tsiapa, N. Katsarakis, Th. Koschny, C. M. Soukoulis, and E. N. Economou, Left-handed metamaterials: The fishnet structure and its variations, *Phys. Rev. B* **75** (2007) 235114

[21] J. Zhou, Th. Koschny, and C.M. Soukoulis, An efficient way to reduce losses of left-handed metamaterials, *Opt. Express* **16** (2008) 11147

[22] C. Garcia-Meca , R. Ortuno, F.J. Rodriguez-Fortuno, J. Marti, A. Martinez, Negative refractive index metamaterials aided by extraordinary optical transmission, *Optics Letters* **34** (2009) 1603

[23] L. Feng, M.-H. Lu, V. Lomakin, and Y. Fainman, Plasmonic photonic crystal with a complete band gap for surface plasmon polariton waves, *Applied Physics Letters* **93** (2008) 231105

[24] Z. Liu, H. Lee, Y. Xiong, C. Sun, X. Zhang, Far-Field Optical Hyperlens Magnifying Sub-Diffraction-Limited Objects. *Science* **315** (2007) 1686

[25] Y. Liu, G. Bartal, X. Zhang, All-angle negative refraction and imaging in a bulk medium made of metallic nanowires in the visible region, *Optics Express* **16** (2008) 15439

[26] A.N. Grigorenko, A.K. Geim, H.F. Gleeson, Y. Zhang, A.A. Firsov, I.Y. Khrushchev, and J. Petrovic, Nanofabricated media with negative permeability at visible frequencies, *Nature* **438** (2005) 335.

[27] A.N. Grigorenko, Negative refractive index in artificial metamaterials, *Optics Letters* **31** (2006) 2483

[28] S. Linden, C. Enkrich, M. Wegener, J. Zhou, T. Koschny, C. M. Soukoulis, Magnetic Response of Metamaterials at 100 Terahertz, Science **306** (2004) 1351

[29] S. Zhang, W. Fan, N. C. Panoiu, K. M. Malloy, R.M. Osgood, and S. R. J. Brueck, Experimental demonstration of near-infrared negative-index metamaterials, *Phys. Rev. Lett.* **95** (2005) 137404

[30] T. J. Yen, W. J. Padilla, N. Fang, D.C. Vier, D.R. Smith, J.B. Pendry, D.N. Basov, Terahertz Magnetic Response from Artificial Materials, *Science* **303** (2004) 1494

[31] S. Linden, C. Enkrich, M. Wegener, J. F. Zhou, T. Koschny, and C. M. Soukoulis, Magnetic response of metamaterials at 100 terahertz, *Science* **306** (2004) 1351.

[32] N. Katsarakis, G. Konstantinidis, A. Kostopoulos, R. S. Penciu, T. F. Gundogdu, Th Koschny, M. Kafesaki, E. N. Economou, and C. M. Soukoulis, Magnetic response of split-ring resonators in the far infrared frequency regime, *Optics Letters* **30** (2005) 1348.

[33] C. Enkrich, S. Linden, M. Wegener, S. Burger, L. Zswchiedrich, F. Schmidt, J. Zhou, T. Koschny and C. M. Soukoulis, Magnetic metamaterials at telecommunication and visible frequencies, *Phys. Rev. Lett.* **95** (2005) 203901.

[34] Y. Ekinci, A. Christ, M. Agio, O.J.F. Martin, H.H. Solak, J.F. Löffler, Electric and magnetic resonances in arrays of coupled gold nanoparticle in-tandem pairs, *Optics Express* **16** (2008) 13287

[35] P. Markos and C. M. Soukoulis, Numerical studies of left-handed materials and arrays of split ring resonators, *Phys. Rev. E* **65** (2002) 036622.

[36] S. Zhang, W. Fan, B.K. Minhas, A. Frauenglass, K. J. Malloy, S. R.J. Brueck, Mid-infrared resonant magnetic nanostructures exhibiting a negative permeability, *Phys. Rev. Lett.* **94** (2005) 037402

[37] C. Rockstuhl, T. Zentgraf, H. Guo, N. Liu, C. Etrich, I. Loa, K. Syassen, J. Kuhl, F. Lederer, H. Giessen, Resonances of split-ring resonator metamaterials in the near infrared, *Appl. Phys. B* **84** (2006) 219

[38] C. Rockstuhl, T. Zentgraf, E. Pshenay-Severin, J. Petschulat, A. Chipouline, J. Kuhl, T. Pertsch, H. Giessen, F. Lederer, The origin of magnetic polarizability in metamaterials at optical frequencies - an electrodynamic approach, *Opt. Express* **15** (2007) 8871

[39] V.V. Varadan and A.R. Tellakula, Effective properties of split-ring resonator metamaterials using measured scattering parameters: Effect of gap orientation, *J. Appl. Phys.* **100** (2006) 034910.

[40] J. Zhou, T. Koschny, C.M. Soukoulis, Magnetic and electric excitations in split ring resonators, *Optics Express* **15** (2007) 17881

[41] N. Katsarakis, G. Konstantininidis, A. Kostopoulos, R.S. Penciu, T.F. Gundogdu, M. Kafesaki, E.N. Economou, Th. Koschny, C.M. Soukoulis, Magnetic response of split-ring resonators in the far-infrared frequency regime, *Optics Letters*, **30**, (2005) 1348

[42] M. Decker, S. Linden, M. Wegener, Coupling effects in low-symmetry planar split-ring resonator arrays, *Optics Letters* **34** (2009) 101579

[43] B. Kante, A. de Lustrac, J.-M. Lourtioz, F. Gadot, Engineering resonances in infrared metamaterials, *Opt. Express* **16** (2008) 6774

[44] N. Liu, H. Guo, L. Fu, S. Kaiser, H. Schweizer, H. Giessen, Three-dimensional photonic metamaterials at optical frequencies, *Nature Materials* **7** (2008) 31

[45] H. Chen, L. Ran,J. Huangfu, X.M. Zhang, K. Chen, T.M. Grzegorczyk, and J.A. Kong, Left-handed materials composed of only S-shaped resonators, Phys Rev E **70** (2004) 057605.

[46] K. Aydin, I. Bulu, K. Guven,M. Kafesaki, C.M. Soukoulis, E. Ozbay, Investigation of magnetic resonances for different split-ring resonator parameters and designs, *New J. of Physics* **7** (2005) 168.

[47] B. Kante, A. de Lustrac, J.-M. Lourtioz, B. Burokur, Infrared cloaking based on the electric response of split ring resonators, *Optics Express* **16** (2008) 9191

[48] C.R. Simovski and S.A. Tretyakov, On effective electromagnetic parameters of artificial nanostructured magnetic materials, *Photonics and Nanostructures - Fundamentals and Applications,* **8** (2010) 254263.

Chapter 3

State-of-the-art and most promising analytical and numerical characterization techniques for nanostructured metamaterials

3.1 Introduction to electromagnetic characterization

In spite of the fast development of nanoscience and nanotechnologies the problem of the electromagnetic characterization of nanostructured materials has been only scantly studied, and methods and techniques of this characterization are barely developed. There are several reasons for this. First, a significant part of known nanostructures are not materials in the common meaning of the term. Nanowaveguides, nanoantennas, nanocircuits [1, 2] and other nanodevices (logical nanoelements and optical memory nanocells, surface-plasmon lasers called SPASERs, etc. [3]) are devices, not materials. The theoretical electromagnetic characterization of these devices (e.g. calculations of the input impedance and pattern of a nanoantenna) does not face the basic theoretical problems. Their characteristic parameters are unambiguous, and only difficulty there is their accurate computation. The attention of specialists in the electromagnetic characterization is strongly attracted to nanodevices and not enough attention is paid to nanomaterials.

As to nanostructured *materials*, the methods of their chemical and structural characterization are well developed, including techniques based on electromagnetic (optical) devices. Chemical characterization of constituents can be done using already classical methods of optical spectral analysis: Surface-Enhanced Raman Scattering (SERS) and fluorescence and luminescence spectral measurements. Electrostatic and magneto-static properties of some nanostructured materials (e.g. the conductivity of arrays of carbon nanotubes [4]) are well studied and there are no theoretical problems with similar characterization of other nanomaterials. However, when the goal is to characterize the *electromagnetic properties* of nanostructured materials, researchers encounter a very basic difficulty. It is, in principle, more difficult to characterize an artificial material than a device because artificial materials are extended heterogeneous structures comprising a huge number of interacting constitutive elements. For a significant part of nanomaterials it is

not only unclear how to calculate (and moreover, how to measure) their electromagnetic characteristic parameters. Even a list of these characteristic parameters has not been conclusively established at present time. One researcher characterizes some nanostructured materials by only dielectric permittivity. Another one claims for the same material some non-trivial permeability. The third proves that both of them are wrong since these parameters applied to those materials have no physical meaning. The fourth researcher asserts that within certain bounds they perhaps can characterize some electromagnetic properties but it is so only if permittivity and permeability are complemented by some additional material parameters...

Even for a specialist in the electromagnetic theory it is sometimes very difficult to judge who of them is wrong and who is right. For example, in many works simple cubic lattices of plasmonic nanospheres are electromagnetically characterized by an only scalar complex parameter – isotropic complex permittivity (e.g. [5,6]). Meanwhile, in some other papers (e.g. [7]) it is noticed that these lattices are photonic crystals, their permittivity is spatially dispersive and therefore cannot be isotropic. Moreover, in [8] the same lattices are characterizes by four tensor material parameters which are all non-zero and non-trivial (i.e., 12 scalar parameters in total). This situation in the electromagnetic characterization of nanostrucrtured metamaterials complicates the writing of the state-of-the-art overviews and makes the choice of the best technique very problematic because these problems are not fully understood at this time.

3.2 Retrieval of material parameters for bulk nanostructures with non-resonant constitutive elements

This is the simplest case of many natural materials and some artificial media, and we discuss this first. As was mentioned above, the response of most isotropic bulk media to an incident plane wave can be described, in the long-wavelength limit, by a frequency dependent electrical permittivity, ε, and magnetic permeability, μ. These can be obtained using the scattering data from a finite slab of such material, considering the material as a homogeneous medium. This approach can be applied for natural and composite media, but fails in two cases. First, it fails when the wavelength becomes comparable to the material unit cell size (practically when the unit cell maximal size a becomes not optically small, for example when it exceeds $\lambda/4$. This situation corresponds to the frequencies close to the first band gap of the lattice, which in this case should be considered as a photonic crystal rather than as a composite medium. In our definition, photonic crystals do not refer to effectively homogeneous materials and consequently are not metamaterials. Second, the standard retrieval procedure fails for MTM at frequencies where the material is resonant.

Consider now the frequency ranges in which the composite material is not resonant. For non-resonant and optically dense ($a < \lambda/4$) composite media the standard approach to electromagnetic characterization can be used. This is so because a layer of such a medium in spite of its heterogeneous internal structure can be considered as being effectively continuous between its physical boundaries. There are two main methods of the experimental electromagnetic characterization of non-resonant composite media. One is the

RT-retrieval method, also called the Nicholson-Ross-Weir (NRW) method, Section 3.3.2. It is also often used for the theoretical electromagnetic characterization of nanostructured materials in numerous works (see discussion below). Another is the modern ellipsometric method called VASE which is probably not applicable to theoretical characterization of composite media, however, it is widely used as a powerful experimental method to characterize nanostructured materials (see e.g. in [26]– [34]). More information on this can be seen in the comprehensive review [9].

3.3 Direct and inverse (retrieval) homogenization approaches

As already indicated, it is of prime importance to define and specify the applicability domain and the physical meaning of every material parameter that is used to characterize a structured material. We recall that only the parameters that describe the material properties in a condensed way consistently and unambiguously can be called characteristic material parameters. The effective material parameters result from a homogenization procedure, however, only adequate homogenization models guarantee that the effective material parameters fit the concept of the electromagnetic characterization, i.e., give an accurate and practically useful condensed description of the material response to electromagnetic waves.

There are two main approaches to the homogenization of bulk lattice structures. One approach can be called direct homogenization. It is a theoretical approach. It starts from the known polarizabilities of individual particles and goes through averaging of microscopic fields and microscopic (local) polarization and magnetization. The result of the averaging in the sense of the averaging of Maxwell equations is a set of material equations (2.5) (or, in the general case, (2.15) and (2.16)) where the EMP are expressed through individual polarizabilities of particles. The relations expressing EMP through polarizabilities of individual particles and other parameters of the original heterogeneous structure are the main results of this direct approach. However, to assess whether these EMP are representative of the characteristic parameters, it is necessary to analyze the properties of waves with different polarizations of the electric field vector, propagating at different directions in the lattice.

At first, the same set of EMP should describe eigenwaves propagating in different directions with respect to the lattice axes. However, this is still not enough – applicability of these EMP to the boundary problems (at least the interface problem for layers) should also be checked. If the same set of EMP is also suitable for describing the wave reflection and transmission at the interface at different angles of incidence, then we can finally conclude that this set of EMP is really adequate and these EMP can be called electromagnetic characteristic parameters of the medium. All these issues have been addressed in the classical homogenization model of natural crystals developed in 1910s-1950s by P. Ewald, S. Oseen, M. Born, D. Sivukhin and others. This model refers to the case when the optical size of the unit cell is very small $|q|a < 0.01$ where q is wave number and a is the lattice constant.

For composite media, especially for MTM which normally operate in the range $0.01 <$

$qa < 1$ a similar thorough theory has not been developed yet. Moreover, many researchers working with MTM (especially, with nanostructured MTM) prefer the inverse approach suggested in 2002 in works [10,11]. This approach can be called heuristic homogenization. In this approach the sample formed by an array of artificial particles in the dielectric matrix is heuristically replaced by a body of the same shape filled with an isotropic uniform continuous magneto-dielectric medium with unknown ε and μ to be determined. The latter two complex quantities are retrieved from measurement or from accurate numerical simulation of two scattering parameters of the body at a specific angle of the wave incidence and wave polarization type (reflection and transmission coefficients). Then it is assumed that the sample composed of the actual MTM will have all scattering characteristics identical to those of the effective continuous magneto-dielectric medium with such ε and μ as were found for the specific case of a particular plane-wave incidence.

Is this approach justified? Any model, even crude, is justified if it is predictive and works in the design of devices. However, the authors of the present report do not know any work, which would prove that ε and μ retrieved in this way for any nanostructured MTM are applicable to all angles of the wave incidence and for both polarizations of exciting waves. On the contrary, from the available literature (see the review in [9]) one can infer that these quantities are in general apparently applicable only to the same case of the wave incidence in which they were retrieved. Therefore they do not fit the concept of the electromagnetic characterization.

This heuristic homogenization was however often claimed successful [9], and this claim has some reasonable grounds. Indeed, works based upon the aforementioned parameter retrieval often refer to a special class of MTM samples, composed of finite-thickness orthorhombic lattices of small resonant scatterers. These scatterers are not bianisotropic and at most frequencies (beyond the ranges of quadrupole and other multipole resonances) they can be adequately modelled by electric and magnetic point dipoles. The finite thickness lattice forms a layer (infinite in a plane and finite in the normal direction) with an integer number N of unit cells across it. Its scattering parameters are complex valued reflection R and transmission T coefficients. The retrieval of EMP from R and T coefficients of a layer of a continuous magneto-dielectric medium is the standard method (called NRW method), which is discussed in Section 3.3.2. In many papers it was found that EMP retrieved for this class of MTM by the NRW method do not depend on N, i.e. they remain unchanged for any layer thickness if divisible by the lattice period $d = Na$. One may conclude that these EMP are representative of the internal properties of the layer because they are independent of the layer thickness, and they characterize the material inside the layer. Formally, this is the case. For a special class of MTM the parameters ε and μ retrieved by the NRW method do indeed comply with the definition of EMP. This class of lattices was called in [12] the Bloch lattices. This name is related to the possibility to easily introduce the so-called Bloch impedance for these lattices. However, even for Bloch lattices these retrieved material parameters unfortunately do not fit the concept of the characteristic material parameters, because the locality limitations are violated for them. This is a clear indication, that the retrieved ε and μ do not fully fit the characterization concept. The non-local parameters obtained for the case of the normal wave incidence cannot be applied to other excitation cases. Even in the case of normal incidence they become inapplicable, if the same MTM layer is mounted on different substrates.

As it is evident now, the locality violation in the retrieved parameters was an indi-

cation, that the heuristic homogenization was flawed, and the prime attention should be paid to alternative (direct and inverse) homogenization models. However, this problem was not duly understood before 2006. The absence of locality in the retrieved parameters of Bloch lattices was interpreted in the numerous papers as a sign of strong spatial dispersion. Meanwhile these media as a rule behave as effectively continuous ones. Locality of the medium response can be easily checked through the frequency dependence of the retrieved refractive index n and wave impedance Z. The two locality limitations formulated above for permittivity and permeability can be also formulated for n and Z. Causality requires growth of the refractive index n with the frequency in the low-loss frequency regions (where the imaginary part of n is negligible). This is called the Foster theorem (e.g., [13]). Additionally, passivity requires the sign of the imaginary part of n and of the real part of Z to be consistent with lossy medium, i.e. positive for the optical selection for the time dependence $\exp(-i\omega t)$ and negative for the engineer selection $\exp(j\omega t)$.

Inspecting many papers devoted to Bloch lattices of small separate (non-bianisotropic) scatterers, it was observed that within the frequency region $|q|a < 1$ locality is satisfied for n and Z and therefore strong spatial dispersion does not occur [9,12,14,15]. Therefore, the non-local material parameters are retrieved because the simplistic inverse homogenization model [10, 11] fails. It was shown in [9, 12, 14, 15] that the failure happens because Maxwell's boundary conditions which are implied by this model can be insufficient for macroscopic fields. Maxwell's boundary conditions are equations of continuity for tangential components of fields $\mathbf{E}$ and $\mathbf{H}$ at interfaces of two different materials. For truly continuous media there is no difference between microscopic and macroscopic fields and these conditions are obviously satisfied. If the medium is formed by strongly dispersive (resonant) particles, these conditions are satisfied only for microscopic fields. For macroscopic ones it is not necessarily the case.

It is therefore clear that new, more advanced, inverse homogenization models for MTM are needed. Unfortunately, progress in the theoretical homogenization of MTM up to 2009-2010 has been very modest. Only a few works are known, which link microscopic theoretical models of nanostructured MTM with a possibility of experimental electromagnetic characterization. As already noticed, in order to find characteristic parameters of an artificial material, its theoretical model has to explicitly include boundary conditions. As a result, it should establish the relationships between material parameters and scattering parameters, which can be experimentally measured, e.g. R and T coefficients of a layer. When measured in the far-field zone, these two coefficients contain only macroscopic (averaged) information about the structure properties. The contribution of evanescent waves which contains microscopic information cannot be uniquely extracted from the far field, i.e., from the reflected and transmitted waves. Only for a special class of MTM – for the Bloch lattices – such incomplete information can be sufficient for their characterization [16]. However, it is not yet fully clear if it is really the case even for these lattices, since the study of their electromagnetic properties for oblique incidence of waves has not yet been done.

3.3.1 Are the retrieved effective material parameters of nanostructured materials representative of their characteristic parameters?

This is the fundamental question which should always be considered in the process of experimental electromagnetic characterization of nanostructured materials (the last step of the scheme described in Section 4.3). The retrieval of material parameters of an effective homogeneous medium evidently implies that we replace the original heterogeneous structure by an equivalent homogeneous medium. In what sense this equivalence can be understood? It is clear that the homogeneous model should imitate the electromagnetic properties of the original inhomogeneous material. But it is also clear that all electromagnetic properties cannot be imitated since the homogenization is always an approximation. So, which properties are important to imitate?

For samples which can have different shapes this is the equivalence of the overall scattering properties which is described in the electromagnetic theory by the so-called scattering matrices. Two bodies of the same shape (one of which is made of the original inhomogeneous structure and the other one of the corresponding homogenized material) should have practically identical scattering matrices. Fortunately, most nanostructured materials are prepared as layered structures and we can consider them as layers of finite thickness, whereas in the interface plane they are practically infinite. Then the equivalence of scattering matrices reduces to the equivalence of reflection and transmission coefficients for plane waves. However, the crucial moment is that this equivalence should hold for any incidence angle, since homogenous material is characterized by material parameters which are invariant with respect to the incident wave propagation direction. Moreover, material parameters of continuous media such as ε and μ obey the basic physical limitations of locality as explained in Section 2.5.5. If the retrieved effective material parameters turn out to be different for different angles of the wave incidence or if they violate fundamental physical limitations, then this homogeneous material model cannot be equivalent to the structure under study.

The retrieved effective material parameters can be obtained wrongly due to several reasons. First, the structure can be spatially dispersive in the frequency range where the retrieval of material parameters is done. Many metamaterials behave as spatially dispersive (effectively discrete) structures within some narrow frequency interval(s) laying inside the resonance band of inclusions but outside this (these) narrow sub-band(s) they behave as continuous media. Then outside these regions it is possible to properly retrieve the effective material parameters which characterize the medium, but within them it is impossible and the retrieved parameters have no physical meaning. Another reason can be a wrong retrieval model. First, the researcher can try to characterize an anisotropic medium by scalar ε and μ. Since the scattering by anisotropic layers obeys different laws than the scattering by isotropic layers, this approach delivers wrong scalar material parameters. Third, if the retrieval procedure which is valid only for natural materials or for composites of non-resonant constitutive elements is applied to arrays of resonant elements, it also delivers wrong material parameters. This situation is most difficult and it is discussed below in more detail.

Usually one retrieves effective material parameters for one angle of incidence and hopes

that they are applicable to other angles. However, these hopes are not always grounded for MTM. Below we present a typical list of indications that the applied retrieval procedures for nanostructured MTM are not adequate for particular structures or frequency ranges:

- Retrieved parameters depend on the sample size and on the surrounding environment (e.g. [26]);
- Retrieved parameters have non-zero imaginary parts in the absence of dissipation (e.g. [27]);
- The sign of the imaginary part of one of retrieved material parameters is opposite to the sign of the other one (e.g. [28]);
- The frequency dispersion of retrieved material parameters violates the causality limitations (e.g. [29]).

In all these cases the retrieved material parameters are non-physical and therefore should be different for different incidence angles (see e.g. in [30]). Therefore they cannot be considered as electromagnetic characteristic parameters.

3.3.2 The standard RT-retrieval method (NRW method)

The RT-retrieval (also called the S-parameter retrieval) is the most commonly used characterization method for nanostructured materials and metamaterials. The name refers to the reflection and transmission coefficients for the normal incidence of the probing plane wave. This is a quite simple procedure, since the transmission and reflection of a plane wave by a homogeneous medium are relatively simple functions of the refractive index, n, and the wave impedance, Z, of the effective medium, whose bulk material parameters can be in their turn found as $\varepsilon = n/Z$ and $\mu = nZ$. The NRW method principally operates by analyzing the transmission and reflection signals for the calculation of the dielectric and also magnetic properties of bulk layers. Its main advantage is that it can be applied in a wide frequency range providing a broadband description of the medium dispersive properties.

Considering the scattering configuration shown in Fig. 3.1, where an incident plane wave of the form $\mathbf{E}_{\text{inc}} = \mathbf{y}_0 E_{\text{inc}} \exp[j(\omega t - kx)]$ impinges normally on a slab of a homogeneous material in vacuum, one can find the refractive index n and the wave impedance Z through measured (or numerically simulated) reflection R and transmission T coefficients of the slab using inverted Fresnel-Airy formulas:

$$\cos(\omega\sqrt{\varepsilon_0\mu_0}nd) = \frac{1 - R^2 + T^2}{2T}, \quad Z = \pm\sqrt{\frac{(1+R)^2 - T^2}{(1-R)^2 - T^2}}. \tag{3.1}$$

Here the transmission coefficient T refers to the back surface of the slab. There are many works on the proper choice of the inverse cosine branch for n and of the sign of the real part of Z (which must be positive in passive media). We do not discuss these details here.

The most important advantage of the NRW method for the theoretical electromagnetic characterization of nanostructured layers is related to the fact that these layers are

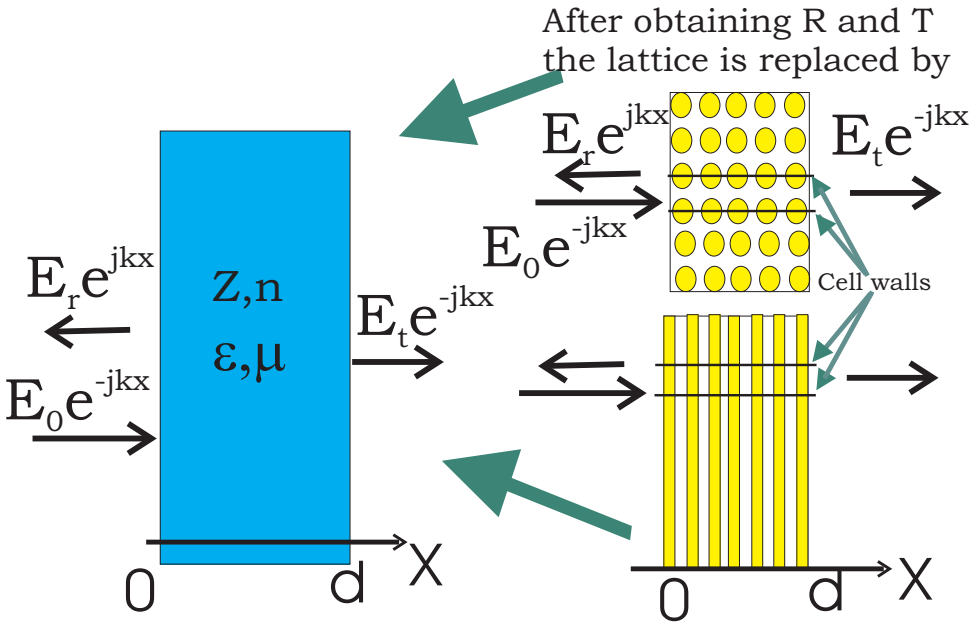

Figure 3.1: The configuration used in the NRW method for the determination of effective material parameters from reflection and transmission data for a non-resonant composite slab. The structure period across the slab is small. The structure can comprise inclusions which are small in all three dimensions (the upper one). Alternatively, inclusions can be extended in the plane parallel to the slab boundaries (the lower one). In the last case one can refer to a partial (conditional) electromagnetic characterization.

periodic. This allows one to perform exact numerical simulations of R and T coefficients using commercially available software. The periodicity in the plane parallel to the layer interfaces yields the boundary problem with the plane wave incidence to the so-called cell problem. Then one can select a unit cell of the structure and ascribe to the cell walls so-called periodic boundary conditions. For a lattice of inclusions which is infinite along one direction, (as it is in the case of the wire medium, for example) the unit cell size can be chosen arbitrary. The periodical conditions at the walls of a unit cell allow one to consider only a single unit cell and to calculate the fields only inside it. In the infinite structure around the selected cell the same fields are periodically replicated. Even if the unit cell contains 10-20 particles, such a problem is not challenging for modern electromagnetic software. One calculates R and T, retrieves from them n and Z using (3.1), and finally finds ε and μ.

Let us conclude this subsection by two important comments. The NRW method implies the normal propagation of the wave in the material slab. Therefore, the obvious condition of optical smallness of the structure period a refers only to the period across the slab. To consider the medium as effectively continuous is possible not only if the slab is formed by optically small inclusions. It can be an array of long inclusions (e.g. wires), if they are parallel to the slab boundary. This possibility seems to broaden the scope of applicability for this method. However, it is not that simple. In fact, the retrieved effective material parameters can be treated as characteristic parameters only in the case when the particles are optically small and isotropic. If the inclusions are not small in the transverse direction, material parameters, retrieved from the measurements of R and

T coefficients for the normal incidence, can be applied for condensed description of the materials only for this particular excitation. For a slab of a wire medium or for a structure of alternating metal and dielectric layers this simple approach is not applicable. Here the oblique propagation of waves obeys different laws than the normal propagation. The interaction of the obliquely propagating wave with such media cannot be considered in terms of the permittivity which was retrieved for the normal incidence. Moreover, in the case of the oblique propagation of the wave such media are spatially dispersive and to relate their effective material parameters to R and T coefficients so-called additional boundary conditions are needed. However, if there is a reliable theoretical model of the structure and a minimal knowledge on its geometrical parameters (e.g. the period a across the slab), the NRW retrieval will be not useless. For example, for a wire medium from the retrieved permittivity one can find the so-called plasma frequency which can be further used for calculating the spatially dispersive material parameters. This case can be referred as partial or conditional electromagnetic characterization.

The second comment refers to the obvious requirement of the absence of resonances of the whole structure. In fact, the NRW method is inapplicable in the frequency ranges of the Fabry-Pérot resonances (the thickness resonances of the slab) (e.g., [31]). At these resonances the method, if applied, leads to difficulties in extracting the effective material parameters even for very simple cases of natural dielectrics.

3.3.3 Ellipsometry techniques

Ellipsometry is a classical optical measurement technique used to experimentally study thin planar layers [32, 33]. Linearly polarized obliquely incident light beams are used to probe the electromagnetic properties of layers, as is illustrated in Figure 3.2.

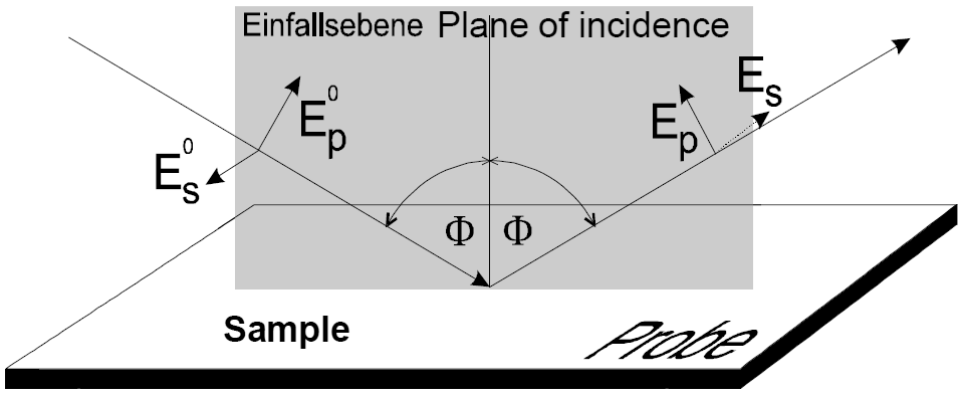

Figure 3.2: Basic ellipsomentry configuration: Reflection of two linearly polarized beams, oblique incidence. Picture from the lecture of K. Hirgerl (http://school.metamorphose-vi.org/images/school-2010-12/Hingerl.pdf).

The polarization plane is chosen so that the amplitudes of the electric fields in the incidence plane (E_p^0, p-polarization) and the field in the orthogonal plane (E_s^0, s-polarization) are equal. Since the reflection coefficients for the two polarizations are different for oblique angles, the reflected beam is elliptically polarized. Moreover, if the layer is lossy or

anisotropic, each of the two orthogonal components of the incident beam creates some cross-polarized reflected waves. The reflection process can thus be characterized by a set of co- and cross-polarized reflection coefficients.

Let us denote by $r_{ss,pp}$ the ratios between the electric fields of the incident and reflected waves of the same polarization and by $r_{sp,ps}$ the ratio of cross-polarized reflected electric field to the corresponding incident field. As it is a serious technical challenge to measure the complex reflection coefficients, the ellipsometry approach goes around this difficulty and measures, instead, the complex *ratio* of the reflection coefficients r_{pp}/r_{ss} at different incidence angles. Most modern set-ups can measure also the reflection amplitudes $|r_{ss}|^2$ and $|r_{pp}|^2$. Generalized ellipsometry measures also the ratios r_{sp}/r_{ss}, r_{ps}/r_{ss} and so on, which allows measurements of material losses and anisotropy in addition to the real part of the permittivity. If the sample is transparent, it is possible to measure the same ratios as well as the amplitudes also for the respective transmission coefficients.

Next, using the macroscopic models for the layer under test (basically, assuming that it is an isotropic or anisotropic dielectric), the permittivity and / or the layer thickness can be derived from the Fresnel formulas [32, 33]. This technique works very well for "usual materials" that indeed behave as layers of bulk, effectively continuous dielectrics, but it runs into the same fundamental problems if the structure needs more advance models to describe its electromagnetic properties.

Among the known modifications of ellipsometric methods the so-called Variable Angle Spectroscopic Ellipsometry (VASE) [34, 35] has been recently recognized as most useful and highly accurate method of experimental determination of material parameters (mainly permittivity) from the data of optical measurements. Measurements are made at several incidence angles of light which results in an improvement in sensitivity and precision because the received data are taken at a variety of optical path lengths. Light is first passed through a monochromator to narrow its spectral band to a desired range before passing through a polarizer. It then strikes the specimen at an oblique angle, reflects onto a second, sometimes rotating polarizer known as an analyzer and is received by a detector. The angle of incidence, which is controlled by a computer, generally varies between 50° and 80° in a rotating analyzer ellipsometer, but this is dependent on the sample type [36].

The spectrometer measures the ratio of the s and p components for different angles and the existing softwares [37] fit the angular dependence of these results to the mathematically generated model of this angular dependence expected for a uniaxial layer of given thickness. This fitting delivers the most suitable values of both components of the complex permittivity tensor at a given wavelength. Since the data is measured over the entire wavelength range the analysis of the frequency dispersion of the permittivity allows one to judge on the applicability of the VASE technique to the given nanostructure. If the dispersion turns out to be non-physical, i.e. violates fundamental physical limitations (Section 2.5.5), the method is not applicable. For natural films it was checked that the VASE retrieval is very accurate even near the absorption peaks where the frequency dispersion of permittivity can be strong [38]. Therefore it should be applicable also for electromagnetic characterization of isotropic and uniaxial nanostructured layers beyond the resonance of its constitutive elements.

3.4 Electromagnetic characterization of bulk nanostructured metamaterials (resonant constituents and other complex structures)

3.4.1 Electromagnetic characterization of bulk nanostructured metamaterials: State-of-the-art in 2010

During the last year the situation has dramatically changed. A new trend in the literature devoted to the bulk material parameters of MTM can be easily noticed if we inspect papers published in 2010. This trend has the following features:

- Scientific groups which have gained extremely high reputation over the world by their theoretical and experimental works (Profs. A. Alu, C. Holloway, Yu. Kivshar, E. Kuester, F. Lederer, G. Shvets, and others) have suggested new homogenization models especially addressed to nanostructured MTM [8, 39–47];
- In these papers the theoretical models have been linked to possible experiments, in other words, algorithms of possible experimental retrieval of effective material parameters have been suggested.
- Special attention has been paid to the applicability of the theoretically retrieved material parameters to other cases of wave propagation. In other words, authors concentrate on those effective material parameters which can be called characteristic parameters, their goal is now the electromagnetic characterization. This is probably the most important feature of the aforementioned papers.

In some recent papers (e.g. [39]) results which had been previously obtained in the field of electromagnetic characterization of nanostructured MTM have been re-visited and analytically criticized. It has been shown that in many cases previously retrieved material parameters of nanostructured MTM with claimed magnetic properties are not applicable for other cases of the wave propagation but only for the case for which they were retrieved, and their physical meaning is not clear. Further, in works by other independent researchers [40–42, 48] the physical effect which makes the NRW method not applicable to MTM has been also noticed and widely discussed. This effect is a jump of tangential components of bulk macroscopic fields at the interface of the resonant material. This jump leads to a significant difference between the surface impedance of the material and its wave impedance[1].

Some researchers in this situation suggested novel algorithms of the retrieval of CMP which are not related to the simulation or measurement of R and T coefficients. For example, methods suggested in refs. [8, 42, 43] refer to the measurements or simulations of the fields inside the metamaterial sample. For example, the wave propagation retrieval method [42,43] appears to be perfect for the theoretical calculation of CMP of MTM, even chiral ones [43], which require an additional tensor material parameter for the description

[1]The surface impedance and refraction index are retrieved by the NRW method and used for finding bulk material parameters.

of their bulk electromagnetic properties. However, the problem appears with the applicability of these CMP to the practical boundary problems since the properties of the surface are not taken into account by this method. In fact, the method delivers only CMP of an infinite lattice, similarly to the earlier results in [12,14]. The set of characteristic parameters retrieved in this way is therefore still not complete and the method in its present form is hardly appropriate for the experimental characterization of nanostructured MTM. A similar drawback can be noticed if we consider the method suggested in [8]. This method also introduces a quite unusual description of any metamaterial, even a resonant artificial dielectric through additional tensor material parameters, whose physical meaning is not fully clear. Another important step forward was done by A. Alu in [46,47], where an additional volumetric material parameter is used to remove the non-physical anti-resonances in retrieved permittivity and permeability. Unfortunately, at this stage this approach does not give a reasonably simple scheme for predicting properties of finite-size samples. Despite some still "missing links", all these recent works are very important as a clear indication of the constructive trend in the literature and hopefully these new methods will be further developed by their authors.

In recent works [44,48] the model of the dynamic homogenization of the infinite lattice of electric and magnetic dipoles suggested (to our knowledge) in work by Simovski [49] and applied for the theoretical electromagnetic characterization of MTM in his further works [12, 14–16] has been strongly developed. Namely, the model was expanded from lattices in which the near-field interaction between adjacent crystal planes is negligible (so-called Bloch lattices) to lattices in which this interaction is significant. In the report [45] A. Alu suggested a modification of the model [49] which allows one to fully remove the small deviation of the lattice material parameters from locality. This deviation occurs in the model [49] in a very narrow frequency range in lossless arrays near the lower edge of the resonance band. In works [12,14,15] this effect was practically eliminated by introduction of small losses. Though recent works [44, 45, 48] do not consider surface effects and the retrieved effective material parameters are not enough to solve boundary problems, they evidence that the theorists have started to understand the importance of the dynamic inter-particle interaction for the proper characterization of MTM.

In paper [40] the algorithm previously suggested by Simovski which takes into account both dynamic interaction effects and surface effects has been improved. Instead of transition layers (suggested some 100 years ago by Drude and revisited by Simovski) the authors suggested their compressed version – sheets of effective electric and magnetic currents which should be introduced at the interfaces of the metamaterial layer. However, in this paper the authors could not satisfy the locality limitations in their retrieval procedure. A possible reason of this is probably the small thickness of the sample for which the surface current sheets interact by near fields and their susceptibilities become mesoscopic. Also, in [40] there is no link to the problem of the oblique incidence which should show that the retrieved effective material parameters are really CMP of this metamaterial.

We consider the appearance of all these important contributions within this recent short period as a key prerequisite of a real breakthrough in the electromagnetic characterization of bulk MTM which we expect in the near future.

3.4.2 Electromagnetic characterization of surface nanostructured metamaterials: State-of-the-art in 2010

A progress in this direction is still modest, and, to our knowledge, it is related only to the study by Simovski and Morits performed in summer of 2010 [50]. Using an example of a bilayer of plasmonic nanospheres this work generalized the method of electromagnetic characterization of monolayer magneto-dielectric metasurfaces (metafilms) suggested in [51, 52]. It has been theoretically demonstrated that the results of this characterization method are suitable for predicting scattering parameters of bilayer metasurfaces. Since the authors considered different angles of incidence and theoretically demonstrated that the retrieved material parameters are applicable for all of them, this is an important step in the characterization of metasurfaces.

However, an important theoretical problem is not yet resolved. The approach [51, 52] does not allow one to take into account the dielectric substrate. The theory is applicable only to grids of particles well distanced from all interfaces. Namely, the minimal distance should be larger than the grid period. Generalization of the approach to the realistic case when the particles are located at a dielectric interface is not an easy task. However, there is a strong need in such a theory and we expect in the near future a breakthrough also in this area.

Bibliography

[1] S. Bozhevolnyi, *Plasmonic nanoguides and circuits*, Pan Stanford Publishing, Singapore, 2009.

[2] M.L. Brongersma, *Surface plasmon nanophotonics*, Springer, Dordrecht, 2007.

[3] *Handbook on Surface Plasmon resonance*, eds. R.L.M. Schassfoort, A.J. Tudos, RSC Publishing, Camdridge UK, 2008.

[4] D.M. Guldi, N. Martin, *Carbon nanotubes and related structures*, Wiley, New York, 2010.

[5] V. Yannopapas, A. Modinos, N. Stefanou, Phys. Rev. B **60** (1999) 5359.

[6] J.E. Inglesfield, J.M. Pitarke, R. Kemp, Phys. Rev. B **69** (2004) 233103.

[7] J. Li, G. Sun, C.T. Chan, Phys. Rev. B **73** (2006) 075117.

[8] C. Fietz, G. Shvets, Current-driven metamaterial homogenization, Physica B **405**(2010) 2930.

[9] C. R. Simovski, On electromagnetic characterization and homogenization of nanostructured metamaterials, *Journal of Optics,* **13** (2010) 013001 (1-22).

[10] S. O'Brien and J.B. Pendry, *J. Phys. Condens. Matter*, **14** (2002) 4035.

[11] D.R. Smith, S. Schultz, P. Markos and C. Soukoulis, *Phys. Rev. B.* **65** (2002) 195104.

[12] C.R. Simovski, Bloch material parameters of magneto-dielectric metamaterials and the concept of Bloch lattices, *Metamaterials* **1** (2007) 62.

[13] R.E. Collin, *Foundations for Microwave Engineering,* Mc-Graw Hill, New York, 1966 (first edition); 1992 (second edition).

[14] C.R. Simovski, S.A. Tretyakov, Local constitutive parameters of metamaterials from an effective-medium perspective, *Phys. Rev. B* **75** (2007) 195111.

[15] C.R. Simovski, Analytical modelling of double-negative composites, *Metamaterials* **2** (2008) 169.

[16] C.R. Simovski, On material parameters of metamaterials (review), *Optics and Spectroscopy* **107** (2008) 726.

[17] A.N. Grigorenko, A.K. Geim, H.F. Gleeson, Y. Zhang, A.A. Firsov, I.Y. Khrushchev, and J. Petrovic, Nanofabricated media with negative permeability at visible frequencies, *Nature* **438** (2005) 335.

[18] A.N. Grigorenko, Negative refractive index in artificial metamaterials, *Optics Letters* **31** (2006) 2483

[19] S. Linden, C. Enkrich, M. Wegener, J. Zhou, T. Koschny, C. M. Soukoulis, Magnetic Response of Metamaterials at 100 Terahertz, Science **306** (2004) 1351

[20] S. Zhang, W. Fan, N. C. Panoiu, K. M. Malloy, R.M. Osgood, and S. R. J. Brueck, Experimental demonstration of near-infrared negative-index metamaterials, *Phys. Rev. Lett.* **95** (2005) 137404

[21] T. J. Yen, W. J. Padilla, N. Fang, D.C. Vier, D.R. Smith, J.B. Pendry, D.N. Basov, Terahertz Magnetic Response from Artificial Materials, *Science* **303** (2004) 1494

[22] S. Linden, C. Enkrich, M. Wegener, J. F. Zhou, T. Koschny, and C. M. Soukoulis, Magnetic response of metamaterials at 100 terahertz, *Science* **306** (2004) 1351.

[23] N. Katsarakis, G. Konstantinidis, A. Kostopoulos, R. S. Penciu, T. F. Gundogdu, Th Koschny, M. Kafesaki, E. N. Economou, and C. M. Soukoulis, Magnetic response of split-ring resonators in the far infrared frequency regime, *Optics Letters* **30** (2005) 1348.

[24] C. Enkrich, S. Linden, M. Wegener, S. Burger, L. Zswchiedrich, F. Schmidt, J. Zhou, T. Koschny and C. M. Soukoulis, Magnetic metamaterials at telecommunication and visible frequencies, *Phys. Rev. Lett.* **95** (2005) 203901.

[25] Y. Ekinci, A. Christ, M. Agio, O.J.F. Martin, H.H. Solak, J.F. Löffler, Electric and magnetic resonances in arrays of coupled gold nanoparticle in-tandem pairs, *Optics Express* **16** (2008) 13287

[26] A.P. Vinogradov, A.M. Merzlikin, *Journal of Experimental and Theoretical Physics* 94 (2002) 482-488.

[27] S.M. Rytov, *Sov. Phys. - JETP* 2 (1956) 466-475.

[28] D.R. Smith, S. Schultz, P. Markos, C.M. Soukoulis, *Phys. Rev. B* 65 (2002) 195104.

[29] J. Zhou, T. Koschny, M. Kafesaki, C.M. Soukoulis, *Photonics and Nanostructures* 6 (2008) 96-101.

[30] C. Menzel, C. Rockstuhl, T. Paul, F. Lederer, T. Pertsch, *Phys Rev B* 77 (2008) 195328.

[31] Kh. Chalapat, K. Sarvala, J. Li, G.S. Paraoanu, Wideband reference-plane invariant method for measuring electromagnetic parameters of materials, *IEEE Transactions on Microwave Theory and Techniques* **57** (2009) 2257.

[32] R.M.A. Azzam and N.M. Bashara, *Ellipsometry and Polarized Light,* Elsevier Science Pub Co (1987).

[33] A. Roeseler, *Infrared Spectroscopic Ellipsometry,* Akademie-Verlag, Berlin (1990).

[34] G.E. Jellison, *Thin Solid Films* **313/314** (1998) 193.

[35] V.S. Merkulov, Optics and Spectroscopy **103** (2007) 629.

[36] J. A. Woollam, B. Johs, C. Herzinger, J. Hilfiker, R. Synowicki, and C. Bungay, Overview of Variable Angle Spectroscopic Ellipsometry (VASE), Part I: Basic Theory and Typical Applications, *SPIE Proceedings* **CR72** (1999) 3-28; Part II: Advanced Applications, *SPIE Proceedings* **CR72** (1999) 29-58

[37] G. E. Jellison, *Thin Solid Films* **450** (2004) 42

[38] J. P. Rolland, *J. Am. Chem. Soc.* (2004) 126 (8), 2322

[39] C. Menzel, T. Paul, C. Rockstuhl, T. Pertsch, S. Tretyakov, F. Lederer, Validity of effective material parameters for optical fishnet metamaterials, Physical Review B **81** (2010), 035320

[40] S. Kim, E. F. Kuester, C. L. Holloway, A.D. Scher, J. Baker-Jarvis, Boundary effects on the determination of metamaterial parameters from normal incidence reflection and transmission measurements, submitted to *IEEE Trans. Antennas Propag.*, available at http://arxiv.org/abs/1009.5927v2.

[41] D.A. Powell, Yu.S. Kivshar, Substrate-induced bianisotropy in metamaterials, *Applied Physics Letters* **97** (2010) 091106

[42] A. Andryieuski, R. Malureanu, A.V. Lavrinenko, Wave propagation retrieval method for metamaterials: Unambiguous restoration of effective parameters, *Phys. Rev. B* **80** (2009) 193101

[43] A. Andryieuski, R. Malureanu, A.V. Lavrinenko, Wave propagation retrieval method for chiral metamaterials, *Optics Express* **18** (2010) 15498

[44] R.A. Shore, R.D. Yaghjian, Electromagnetic waves on partially finite periodic arrays of lossless or lossy penetrable spheres, *IEICE Transactions on Communications* **E91.B** (2010) 1819

[45] A. Alu, Spatial and frequency dispersion effects in the homogenization of metamaterial arrays, Abstracts of Metamaterials'2010, Karlsruhe, Germany, September 16-19, 2010, (invited talk)

[46] A. Alu, First-Principle Homogenization Theory for Periodic Metamaterial Arrays, arXiv:1012.1351v1, 6.12.2010.

[47] A. Alu, Restoring the Physical Meaning of Metamaterial Constitutive Parameters, arXiv:1012.1353v1, 6.12.2010.

[48] A.D. Scher, E.F. Kuester, Boundary effects in the electromagnetic response of a metamaterial in the case of normal incidence, *Progress In Electromagnetics Research B* **14** (2009) 341

[49] C.R. Simovski, S. He, Frequency range and explicit expressions for negative permittivity and permeability of an isotropic medium formed by a lattice of perfectly conducting Omega-particles, *Physics Letters A* **311** (2003) 254

[50] D. Morits, C. Simovski, Electromagnetic characterization of planar and bulk metamaterials: A theoretical study, *Physical Review B* **82** (2010) 165114

[51] E.F. Kuester, M.A. Mohamed, M. Piket-May, C.L. Holloway, Averaged transition conditions for electromagnetic fields at a metafilm, *IEEE Trans. Antennas Propag.* **51** (2003) 2641

[52] C.L. Holloway, A. Dienstfrey, E.F. Kuester, J.F. O'Hara, A.A. Azad, A.J. Taylor, A discussion on the interpretation and characterization of meta-films/metasurfaces: The two-dimensional equivalent of metamaterials, *Metamaterials* **3** (2009) 100

Chapter 4

Overview of the state-of-the-art and most promising measurement techniques

4.1 Experimental electromagnetic characterization of metamaterials

Experimental characterisation of metamaterials is predominantly based upon the measurements of the scattering characteristics of the specimens illuminated by plane electromagnetic waves in optical, THz and microwave spectral ranges. Artificial nanostructured materials exhibit strong resonant response to electromagnetic frequencies in the optical part of the electromagnetic spectrum, thus, optical measurements are of prime interest for this overview. Here we discuss measurement techniques for experimental characterization of electromagnetic parameters of nanostructured materials, mainly in the optical part of the spectrum.

4.1.1 Introduction

The field of artificial and nanostructured electromagnetic materials has seen rapid and expansive growth in recent years. As the new and emerging materials advance and become increasingly complex, both the measurement techniques and the material parameter evaluation procedures also evolve to ensure the physically meaningful characterisation and description of the observed phenomena. The integrity and quality of these measurements are of utmost importance here, and therefore it is essential that the appropriate measurement techniques are employed for evaluating the extrinsic response and testing the intrinsic properties of material specimens.

Before directly addressing the metamaterial characterization issues, it is necessary to remark that on the notion of the "optical wavelengths". In the literature it is not strictly defined, but in the bulk of the literature it is understood as the frequency region including infra-red, visible, and ultra-violet frequencies. This corresponds, roughly, to the range of frequencies from 3 THz to 30 PHz (PetaHertz=10^{15} Hz). In terms of the

wavelength, this is equivalent to the range from 0.1 mm to 10 nm. In general, "optical" refers to electromagnetic radiation that can be influenced by lenses and gratings. At lower frequencies, approaching the far-infrared (or the "THz regime"), the issues of sample characterization tend be somewhat different from the optical regime. The visible part of the optical spectrum is between approximately 400 THz (red) to 790 THz (blue) or from 390 nm (blue) to 760 nm (red). At frequencies higher than the visible light, the required inhomogeneity scale becomes too small to be technologically feasible at present, and there are no artificial electromagnetic materials that would function at ultra-violet frequencies.

Also it is instructive to briefly recall how today's state-of-the-art metamaterials at optical frequencies look like – as this aspect poses the relevant constraints to the characterization process. The vast majority of metamaterial structures have been made via serial, hence time-consuming, lithographic approaches (e.g., electron-beam lithography, focused-ion-beam lithography, or direct laser writing). As a result, typical sample footprints are only of the order of 100×100 μm^2. This limited sample size, with respect to the source and detector area at shorter wavelength of measurement leads to use of focusing lenses and the unavoidable averaging of the measurements. This is further discussed in Section 4.1.5. Rather recent brief [1, 2] and comprehensive [3] reviews of the corresponding magnetic and/or negative-index metamaterials can be found in the literature. Examples of notable exceptions are metamaterials made via holographic lithography [4,5] or nano-imprint techniques [6]. The footprint of the latter specimens is of the order of square-centimetres. Yet much larger footprints can be realized along these lines in the future, and there are attempts to use some self-assembly techniques to fabricate metamaterial structures [7–9].

Furthermore, the vast majority of metamaterials at optical wavelengths demonstrated experimentally thus far contain only a single functional layer [1–3], which can contain more than one physical layer. Notable recent experimental exceptions are a three-functional-layer negative-index metamaterial at 1.4-μm wavelength [10], a four-functional-layer magnetic metamaterial at 3.7-μm wavelength [11], and a ten-functional-layer negative-index metamaterial at 1.8-μm wavelength [12]. All of these have a total thickness significantly less than one wavelength of light in free space. Interesting metal-insulator-metal slot waveguide structures supporting backward waves over many wavelengths of light along the propagation direction in the waveguide plane have also been reported [15, 49]. However, their optical characterization is not discussed here as such waveguides are not classified as "metamaterials". There has recently been a concerted effort to push the magnetic frequency response of metamaterials deeper into the visible range of the electromagnetic spectrum. Previous work has shown that simply scaling the size of metamaterial structures, such as split ring resonators (SRRs), only continues to decrease the wavelength of the LC resonance peak up to a certain threshold [50]. Therefore continually making structures smaller in size will not result in the resonance being shifted further and deeper into the visible range.

It is important to note that all the actually fabricated optical metamaterial structures published to date are anisotropic, often they are even biaxial and bi-anisotropic. These geometric variations in the metamaterial parameters further complicate the measurements and analysis effectively multiplying the problem by the number of unique directions in the metamaterial. Furthermore, essentially all metamaterial structures are mechanically supported by some kind of a dielectric substrate – an aspect, which has to be accounted

for in the characterization process as well.

The experimental characterisation of metamaterials is predominantly based upon the measurements of the scattering parameters of specimens illuminated by plane electromagnetic waves in optical, THz and microwave spectral ranges. Therefore, the acquired data are dependant on the angle of incident light and polarization, while most measurements are limited to normal incidence. For measurements using an oblique incidence, the specimens would usually comprise multiple functional layers rather than a single layer structure, which poses numerous fabrication difficulties. For these reasons most experimental works use light at normal incidence.

Additionally, it occasionally is necessary to perform experiments that distinctly measure the electromagnetic interaction between individual constituent elements and particles in the arrays representing the artificial material. Parameters such as the separation distance between structures and layout configurations and geometries have been shown to influence the coupling effects [51], the importance of which has been documented in [52]. For these purposes, near field optical spectroscopy is usually used. Alternatively, a sensitive spatial modulation technique based upon the experimental measurements of the extinction cross-section spectrum has recently been demonstrated for SRR dimmers at near-infrared frequencies.

An EU sponsored publication [16] covers the basic electromagnetic theory and fabrication methods involved.

4.1.2 The ideal measurement

The conceptually perfect experiment on a periodic metamaterial with regular sub-wavelength lattice constant can provide measurements of the frequency-dependent complex reflectance and transmittance coefficients of the sample at all incidence angles and polarizations of the impinging ideal monochromatic plane wave. Furthermore, this ideal measurement should include the (generally elliptical) polarization state of light scattered by the sample. Clearly, in linear optics, frequency-domain information can equivalently be expressed in the time-domain, where "complex" translates into amplitude and phase of the wave. For imperfect or for (intentionally) non-periodic or nonuniform structures, scattering of light into the entire solid angle may occur because the material properties vary across the sample. In the ideal experiment this scattering should be characterized completely for all solid angles.

The raw data acquired in these experiments are subject to further post-processing. However, it is important to emphasise that anything beyond the specific measured quantities, e.g., retrieval of whatever *effective* optical parameters (refractive index, impedance, dielectric permittivity, magnetic permeability, bi-anisotropy parameter, etc.), is not a subject of the experimental optical characterization procedure itself but a subject of *interpretation* (!) of the acquired experimental data. This distinct step - which is interlinked with the parameter retrieval through the theoretical models or numerical simulations - will be briefly discussed in Section 4.2 below. The issues of nonlinear metamaterial characterisation, for example those with gain, are beyond the scope of this review.

4.1.3 Optical measurement techniques

The basic optical measurements (which typically do not provide phase information) can be performed in many analytical laboratories. However the standard instruments may need some modifications to accommodate samples of small size - typically with addition of a microscope optically coupled to the measurement system. The typical setup includes grating spectrometer, in which a broadband light source illuminates slits and light impinges onto a grating which selects only a narrow band of light. Fourier Transform Spectrometer (schematically shown in Figure 4.1) and broad-band ellipsometers in which polarised light is incident at an angle to the substrate surface and the subsequent reflected beam's polarisation state is measured (see Figure 4.2). Some systems allow both transmission and reflection measurements by simple reconfiguration, ellipsometers typically allow the angle of incidence to be varied. However, most commercial spectrometers do not allow the angle of incidence to be varied.

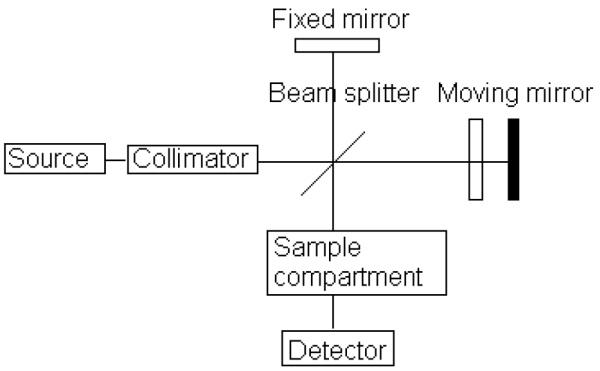

Figure 4.1: Schematic diagram of a Fourier-transform spectrometer. The interference pattern at the detector is obtained by moving the mirror and changing the optical path length. When a sample is present the interfence pattern, as a function of path difference, is modulated by the presence of absorption bands in the sample. The interference pattern is then 'Fourier transformed' to give the absorption (or reflection/transmission) as a function of wave number to give a spectrum [17].

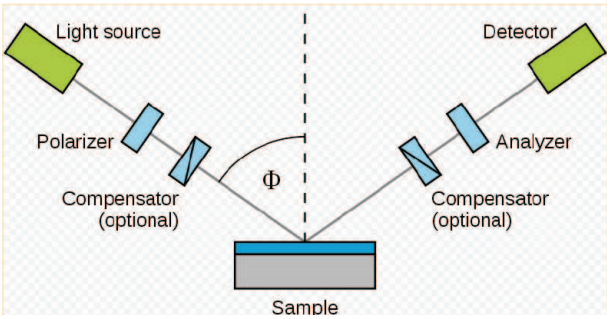

Figure 4.2: Schematic representation of an elipsometer [18].

Similarly, Time Domain Spectroscopy (TSD) in which the phase angle of the measured quantity is obtained from interference methods are usually custom built systems. A simplified schematic of a TDS is shown below in Figure 4.3. The illuminating EM radiation

is generated by the femtosecond pulses from a Ti Sapphire laser incident on either a crystal converter or optoelectronic converter to produce for example THz radiation. The optical delay line alters the phase of the beam arriving at the sample. A detailed introduction is given in reference [19].

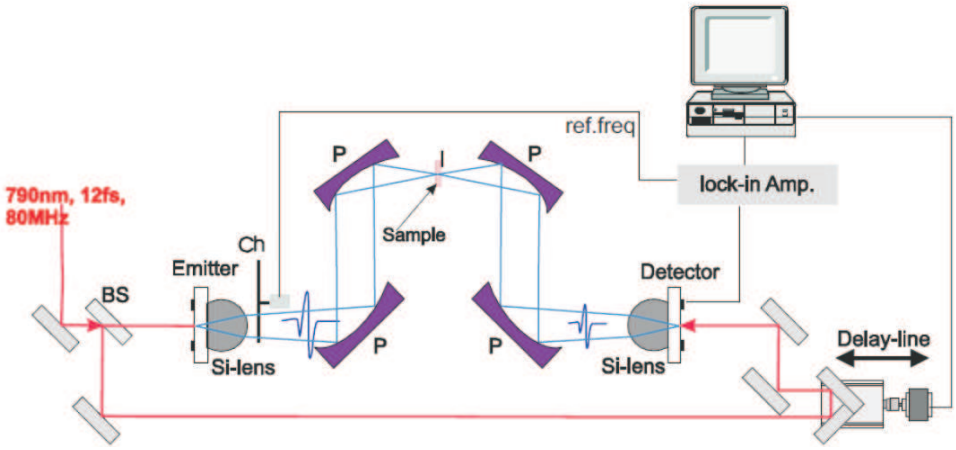

Figure 4.3: Schematic of Time Domain Spectroscopy set-up [19].

4.1.4 Recent advances in measurement techniques

Although no new fundamental ways for metamaterial measurements have been discovered yet, significant progress in S-parameter measurement techniques, particularly in relation to the phase measurements across the spectrum from visible to microwave region, and optical field measurements have been reported recently.

- An experimental method for broadband phase measurements based upon a white-light Fourier-transform spectral interferometer was implemented in [20]. The experimental setup is a Jamin-Lebedeff interferometer modified for the transmission and reflection measurements at normal incidence. The measured data are used to determine the dispersion relation of metamaterials at normal incidence in terms of the complex wavenumber that leads to retrieval of an effective refractive index. Using this approach the refractive index error of the order of 4% in the real and imaginary parts can be achieved.

  The measurements were performed with a supercontinuum light source (spectral bandwidth 0.4 μm – 1.7 μm). After a collimator and a polarizer, the linear polarized light passes a calcite beam displacer, where the beam is divided into two parallel, orthogonally polarized beams with a displacement of 4 mm. These two beams represent the two arms of the interferometer. In the configuration for the transmission phase measurements the beams traverse the sample and then pass an achromatic half-wave plate, which rotates the polarization in each beam by 90°. The two beams are recombined in the second beam displacer. As the beams in the interferometer arms are orthogonally polarized, the interference between them can be obtained using another linear polarizer. Finally, the light is collected into a

photonic crystal (PhC) single-mode fiber and measured with an optical spectrum analyzer.

- THz-Time Domain Spectroscopy (TDS) normally requires two measurements [21]: (i) the waveform is measured for the known reference dielectric material, and (ii) the measurement is made with the test sample. By virtue of reasonably clear separation in time between the main transmitted pulse and the first internal reflection, it is possible to extract only the first directly transmitted THz pulse. Comparing the magnitude ratio and phase discrepancy between the test and reference samples, the real and imaginary parts of the effective refractive index of the sample can be retrieved simultaneously. A detailed retrieval procedure enables one to extract the negative refractive index of low-loss metamaterials based on THz-TDS measurements [21]. The method provides a direct and simple way to probe the real part and imaginary part of refractive index of metamaterials. Its validity has been demonstrated through theoretical simulations on several typical cases.

- At optical frequencies, it is very difficult with the current technology to measure directly the electric and magnetic fields of electromagnetic wave in real time as one cannot measure amplitudes and phases within a single wavelength. Therefore indirect approaches have been developed to obtain the spatial profiles of the guided modes in nanostructured materials. For example, the spatial profiles of all modes have been obtained using spatial Fourier transforms applied to periodic PhC with arbitrary combination of propagating and evanescent waves [53].

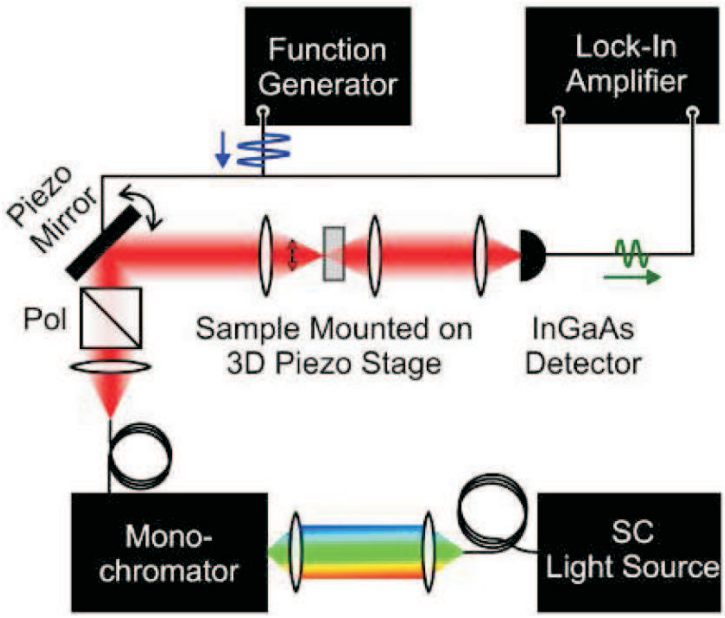

Figure 4.4: A schematic of the experimental spatial modulation equipment setup [54].

The lateral electromagnetic coupling and the corresponding spatial profiles of resonances in SRR dimmers [54] and gold nanoparticles [55] have been obtained by measuring the extinction cross section spectrum and optical absorption. In [54] the extinction cross-section spectrum of SRR dimers (SRRs aligned in various formations) has been measured at near-infrared frequencies using a sensitive spatial

modulation technique. By applying Lorentzian fits to the measured data the resonance frequency, extinction cross-section spectral peak and quality factor were derived. The approach used for the spectral measurements is of primary interest here. A schematic of the spatial modulation setup is shown in Figure 4.4. A white laser beam is passed through a grating monochromator with a resolution of 1nm, filtering the spectrum, before being spatially filtered by a single-mode optical fibre. The output from this fibre is then projected onto the sample to be measured by both a plano-convex and a convex lens separated by a polarizer, thus ensuring linear polarisation of incident light. A piezoelectric tilt mirror is positioned in front of the polariser to modulate the lateral position of the Gaussian beam so that it is on the same plane as the sample, which is itself mounted on a Piezo stage. An InGaAs detector directly connected to a lock-in amplifier is used to detect the light transmitted through the sample.

This is one of the applications of this type of experimental measurement setup. As already mentioned, in the earlier study this technique was utilised to measure the optical absorption of gold nanoparticles, some with a diameter as small as 5 nm [55].

- Direct mapping of the electromagnetic near-fields in metamaterials has recently been reported in [56]. Using experimental setup shown in Figure 4.5, the authors measure the amplitude, phase and polarization of the electric field from a metamaterial made of SRR arrays. Photoconductive antennas emit THz pulses which are optically gated by a connected mode-locked laser. The resultant beam is then imaged onto the metamaterials sample, behind which is a silicon-on-sapphire detector chip. Raster scanning the detector chip, which sits at a distance of 30 μm from the sample surface, allows the THz electric near-field to be spatially resolved. This is made possible by a 10 μm photoconductive gap that lies between H-shaped electrodes that sit on the surface of the silicon. The SRRs on the sample must be positioned closely to the detector electrodes for measurements to be taken. A detailed schematic of the terahertz near-field system and a cutaway profile of the sample and detector chip are shown in Figure 4.5.

  It is noteworthy, that this approach has only been applied to structures in the low terahertz range. The SRRs used in this experiment each had a typical footprint of 500 μm by 500 μm. Nevertheless it is claimed in [56] that this is a rare experimental study in a field dominated by simulation based measurements.

- A novel perspective on optical measurement – the probing of light itself, has been reported in [57]. The experimental setup intended to visualise the electric and, more interestingly, the magnetic field distribution of propagating light is shown in Figure 4.6. A near-field aperture probe with a diameter of 230 nm is used to raster-scan the sample Si_3N_4 waveguide which is connected to linearly polarised laser light with a wavelength of 1550 nm. The probe is positioned only 20 nm above the sample, allowing the retrieval of the evanescent field of the light. The output from the probe is then connected to a reference beam of light, which is laterally split by a polarizing beam splitter for separate detection of electric and magnetic fields. For the magnetic field to be probed and measured, it must first be converted to an electric field so that it can be measured by the detector. This is accomplished by creating a 40 nm

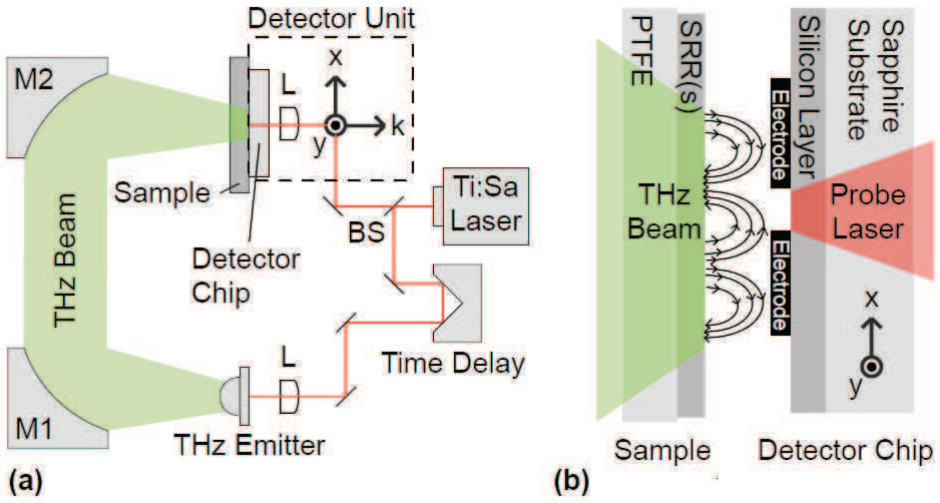

Figure 4.5: (a) Experimental equipment configuration containing a mode-locked laser, beam splitter, lenses, THz emitter, mirrors and detector unit. (b) A cross section of a sample under investigation and the detector chip [56].

crevice in the tip of the probe for optical bi-anisotropy to be exhibited. Because the split is far smaller than the wavelengths of the visible spectrum, electric field signals are suppressed. A similar near-field study into magnetic responses, this time when applied to SRRs, has also been conducted in [58].

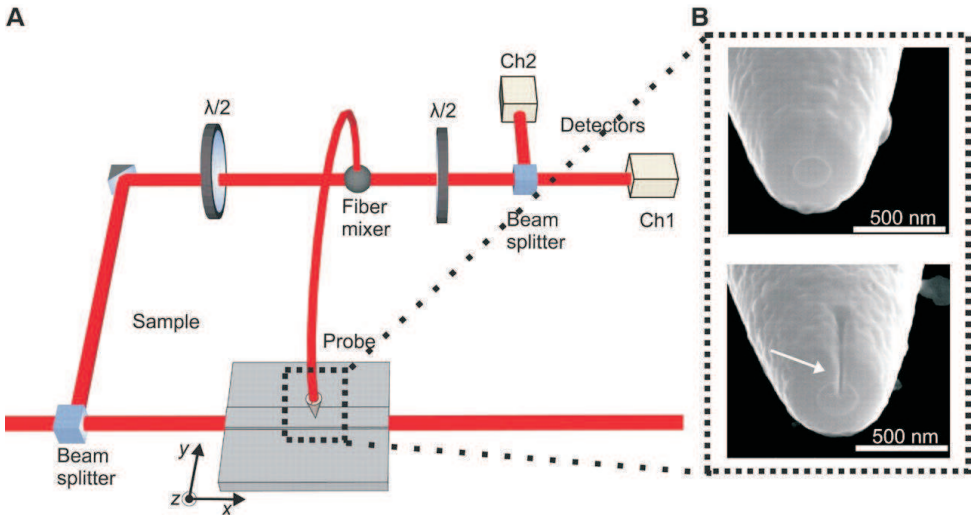

Figure 4.6: (a) Schematic of the experimental setup. (b) Scanning electron micrographs of the two probes used during experimentation - one cylindrical with aperture and the other showing an air gap emanating from the aperture [57].

Despite the fact that such experiments are reliant on interpretation and occasionally modelling of the data acquired, they can prove useful for future advances in optical characterisation. The work detailed in [57] has potential to be of particular benefit for characterisation of metamaterials.

The cited papers discuss various aspects of measurement of a specific nanostructure or metamaterial. Even though some works are based on simulated experiments, they provide insight in the directions where nanostructure fabrication and characterisation are progressing.

4.1.5 Instrumental limitations

At optical frequencies, it is still very difficult with the current technology to measure the electric and magnetic field components of the electromagnetic wave directly versus real time as one cannot easily measure amplitudes and phases within one wavelength. The near-field optical spectroscopy and field mapping suffer from the electromagnetic coupling between the samples and the metallic measuring tip of the apparatus. This implies that the optical response is likely to be distorted [59]. The ability to use far-field techniques to optically detect nanostructures is therefore of great importance for performing measurements unaltered by the influences of test fixtures and measurement instruments.

Therefore the frequency-domain based far-field techniques are primarily employed. Usually, grating spectrometers or Fourier-transform spectrometers merely deliver the intensity of light versus wavelength or frequency. However, all phase information is lost here. Using interferometric techniques, phase information can be (partially) recovered. Commercially available ellipsometers promise to deliver optical constants of thin-film samples but in fact measure angle resolved reflectance polarisation data and rely on idealised models to retrieve the optical constants. Extreme caution should be exercised at this point, because the built-in post-processing software employed for analyzing (or, more precisely, interpreting) these data is limited to the models of dielectric materials and layered structures only. But it is usually inapplicable to deal with magnetic responses (or negative refractive indices). Also, analysis of the low symmetry of metamaterial samples can be problematic here too.

Due to the small lateral footprint of typical samples limited by the present fabrication processes, the incident light wave needs to be spot focused onto the specimen. If the source illuminates the sample edges and surrounding area, the measurement data will be contaminated by response of the other materials in the system. Once a lens is introduced, it concentrates the light from the lens aperture onto the sample at the expense of averaging over the half angular width of the sample seen from the lens aperture (defined as the numerical aperture, NA). This clearly introduces an undesired spread of the incident wave vector components of light, i.e., the experimental results are effectively averaged over a certain range of incidence angles, obviously leading to obscured data. The impact of that averaging process depends on the specific metamaterial under study. For example, it is quite common to image the samples by means of a microscope. As large spectral bandwidths have to be investigated often, reflective microscope objectives are mandatory in order to avoid chromatic aberrations that would otherwise occur for glass-based lenses. It is well known that such Cassegrain objective lenses essentially cut out the normal incidence contribution and average over a cone of incidence angles (e.g., between 15° and 30° with respect to the surface normal for a numerical aperture of $NA = 0.5$). Again, the impact of these "artefacts" needs to be evaluated for each metamaterial structure

separately. A sample that matches the source and detector areas and an arrangement that ensured all the scattered light is collected would constitute an ideal measurement.

Measuring broadband intensity transmittance and reflectance spectra with incident circular polarization of light is far from a trivial task. Broadband linear polarisers are readily available in most spectral ranges and a quarter-wave plate can turn this linear polarization into circular polarization. However, a usual quarter-wave plate has obvious inherent wavelength dependence. At optical and near-infrared frequencies, so-called super-achromatic quarter-wave plates are commercially available. At mid-infrared frequencies, such super-achromatic quarter-wave plates have to be custom-made that incurs significant cost. Also, these structures cannot always be easily integrated into existing (commercial) instrumentation setups. At THz and microwave frequencies, to our knowledge, such super-achromatic quarter-wave plates are presently unavailable at all.

4.2 State-of-the-art in experimental characterisation of metamaterials

All experiments published to date have been far away from the ideal conceptual arrangements described in Section 4.1.2. Several different techniques are usually adopted for the experimental characterisation of metamaterials. The typical approaches are overviewed here.

4.2.1 Structures with inversion symmetry along the surface normal

Suppose that the metamaterial structure exhibits inversion symmetry along the surface normal. In this case, at normal incidence, the reflectance and transmittance spectra do not depend on which side of the sample is illuminated. A quite common procedure is to measure intensity transmittance and/or reflectance spectra of a metamaterial slab of thickness L for normal incidence of light and for two relevant (i.e., linearly independent) incident polarizations, either linear or circular. Clearly, these data containing two quantities at each wavelength are insufficient to retrieve uniquely the optical parameters, e.g., the complex refractive index and the complex impedance of the equivalent isotopic slab at each wavelength. Thus, usually, the experimental data are compared with the theoretical calculations for the designed specimen using additional information on the geometrical parameters which are obtained from optical and/or electron micrographs of the metamaterial samples. If sufficiently good agreement between experiment and theory is obtained, one may apply the theory to compensate for missing experimental phase information.

One way of further analyzing/interpreting the experimental data is to model a fictitious slab of thickness L (with or without substrate) that has exactly the same complex reflectance and transmittance spectra as those of the metamaterial specimen. This "retrieval" procedure (see, e.g., review [3] for discussion of selecting the proper branches of non-unique solutions arising in this process) delivers the two complex quantities for the effective refractive index and impedance, or, equivalently, the effective complex dielectric permittivity and magnetic permeability of the slab. While this procedure is fairly

well defined and broadly adopted in many laboratories around the world, one should be cautious in interpreting these retrieved quantities. Namely, they do represent the optical properties of the metamaterial slab with thickness L - yet they do not necessarily constitute the "material" properties in the conventional sense. One might be tempted to take the knowledge from normal optical materials and transfer it to metamaterials. For example, if one followed the retrieval procedure described above for a thin film of silica (SiO_2) of thickness L, it is clear that the measurements of the same film but of thickness $2L$ would give nearly identical material parameters. This is very often not (!) the case for metamaterial samples. Generally, (near-field optical) interactions between different functional layers of the metamaterial can alter the effective "material parameters". Whether or not this is a significant effect needs to be evaluated for each metamaterial structure under investigation – there is simply no universal answer. Two published experiments at optical frequencies that have addressed this issue [10, 12], and have come to the conclusion that these interaction effects are not too strong for their conditions (both are several layers of double fishnet negative-index metamaterials). A striking counter-example is in ref. [11], where the strong coupling between adjacent layers of split-ring resonators has tremendously altered the properties of a single layer. Yet, the answer to this question also depends on how strongly the layer proximity influences the structure response. For example, it is known from (dielectric) photonic crystals that, for certain aspects (e.g., slow group velocities), the slab thickness exceeding even 100 lattice cells may be insufficient to reproduce the behaviour predicted by the band structure calculations for the fictitious infinite "material".

4.2.2 Structures with no centre of inversion along the surface normal

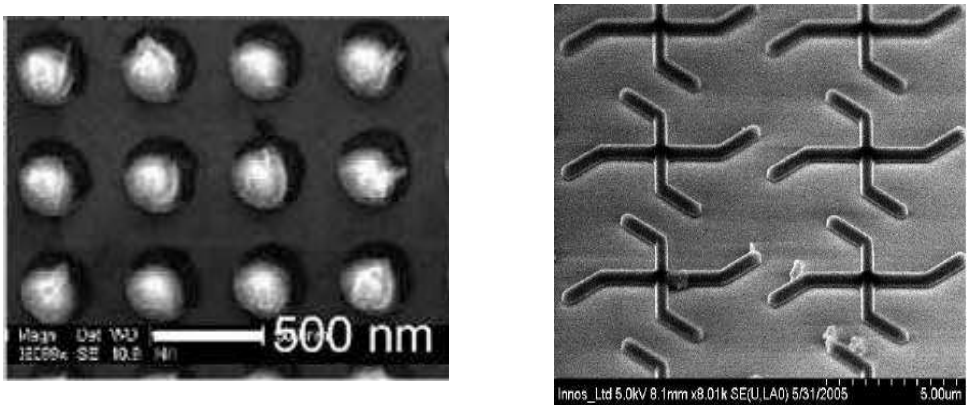

Figure 4.7: (left) - a metamaterial with the centre of inversion (a multilayer array of plasmonic nanospheres prepared in nanogrooves) [13]. (right) - a metamaterial with no centre of inversion (a multilayer array of gammadion-shaped slots performed in the nanofilm of noble metal [14]. Every nanofilm is placed on a dielectric substrate).

The situation becomes more complex if the metamaterial structure has no centre of inversion along the propagation direction of light. Such a metamaterial is shown in

Figure 4.7 in contrast to a spatially symmetric metamaterial. Still restricting ourselves to normal incidence of light onto the metamaterial slab, the complex transmittance and reflectance spectra are no longer the same for the two opposite directions of incidence. In other words, generally eight different quantities have to be measured at each wavelength – provided that the polarization state of the incident light is conserved in both reflectance and transmittance. Otherwise, the number of independent optical parameters doubles. In case of reciprocal structures (i.e., no static magnetic bias applied and there is no natural magnetic phase), the complex transmittances are strictly identical for both directions of propagation, whereas the respective complex reflectances may differ. This amounts to six parameters at each wavelength. Again, in the published optical experiments, not the full fields but only the corresponding intensities have been measured. As a result, the problem of the effective parameters' retrieval is underdetermined. As discussed in Section 4.2.1, additional theoretical input is usually used for extracting the effective optical parameters. One possible approach here is to retrieve the two complex impedances for each side of the equivalent slab at opposite directions of incident waves and a single complex refractive index. Alternatively, the complex permittivity and permeability as well as the bi-anisotropy parameter can be retrieved. Experimentally, this has been done in the literature only once so far in [20]. Needless to say that the meaning of these quantities is subject of the same constraints as in Section 4.2.1, i.e., caution has to be exercised in interpreting these effective quantities as the "material" parameters. They do, however, have a well defined physical meaning for the measured film of thickness L. A variant of the latter approach is proposed in [25] to replace the bi-anisotropy parameter by a wave-vector dependence of permittivity and/or permeability.

4.2.3 Interferometric experiments

Additional information can be obtained from normal-incidence interferometric experiments that – at least partly – recover the missing phase information discussed above. Corresponding publications include Refs. [4, 26–28]. These additional inputs provide further sensitive tests of the level of agreement between the experiment and theory. In that sense, they are very important. However, these additional experimental data do not at all change the conceptual issues of Section 4.2.1.

4.2.4 Oblique incidence

The situation becomes even more complex at oblique incidence of light onto the metamaterial slab. For usual optical materials, generally all optical quantities become tensors of rank three. Only very few experiments on metamaterials at optical frequencies have addressed oblique incidence of light [29, 30]. These papers have just reported the measured transmittance intensity and/or reflectance spectra at different inclination and azimuth angles, but the authors have completely refrained from relating these measurement data to the effective "material" parameters. Theoretical aspects of the respective retrieval procedures are addressed in the literature, see, e.g., [31, 32].

4.2.5 Chiral metamaterials

Lately, progress has been achieved in manufacturing uniaxial chiral metamaterials operating not only at microwave frequencies [33], but also at THz [34] and optical frequencies [35]. Chiral structures are a subclass of bi-anisotropic structures. In bi-anisotropic structures, magnetic-dipole moments can be excited by the electric-field component of the light field and vice versa. In contrast to the general case of bi-anisotropy, where, e.g., the magnetic-dipole moments and the exciting electric field can include any angle, in isotropic chiral media they are parallel. In lossless media this leads to a pure rotation of any incident linear polarization of light, i.e., to optical activity.

Microwave measurements of chirality parameters of natural and artificial chiral materials is a well-established technique. An overview can be found e.g. in [36, Ch. 7]. Transmission-reflection measurements both in free space and in waveguides have been used for this purpose. Small samples (compared with the free-space wavelength) can be measured also using microwave resonators (perturbation analysis is then used to extract the effective parameters). In more recent literature, a detailed theoretical explanation of how the effective parameters can be retrieved from measured data has explicitly been given in Ref. [37].

Recently, corresponding optical experiments have been performed for chiral metamaterial samples. In Refs. [33, 34] effective material parameters have actually been retrieved from the normal-incidence experimental data, while in Ref. [35] different approach was employed. A detailed theoretical explanation of how the effective parameters can be retrieved from measured data has explicitly been given in Ref. [60]. Notably it was found that in contrast to the general bi-anisotropic case, reflectance and absorbance here do not depend on which side of the sample they are taken under normal incidence. Notice, that the structure shown in Figure 4.7 is chiral though the scatterers (bianisotropic slots in the nanofilm) are planar and as such have no asymmetry along the normal direction. The chirality appears here due to the near-field interaction between the scatterer and its dielectric substrate (it vanishes if the substrate thickness tends to zero).

The results of [33, 34] have been discussed in a publication aiming at a broad general readership in ref. [38] (also see references cited therein). An interesting aspect of these latest results is that, for sufficiently strong chirality, a negative phase velocity of light can be obtained even if, in principle, the dielectric permittivity and the magnetic permeability are positive at the same time [39–41].

Provided that phase information is acquired (see above), the measurements can be performed equivalently either with linear or with circular polarization of the incident light. In Ref. [33], phase-sensitive transmittance and reflectance spectra have been taken with linear polarization of the incident light. In Ref. [34], phase sensitive time-resolved data have been Fourier transformed. In both cases, data have to be taken for different linear polarizations as three complex parameters (dielectric permittivity, magnetic permeability, and chirality parameter shall be retrieved). If no phase information is obtained (i.e., only intensity measurements combined with theory), a minimum requirement for meaningful parameter retrieval is that one checks that the two incident circular polarizations of light stay circular (with the same handedness) upon transmission. Furthermore, following the generalized Fresnel coefficients, left-handed circular polarization has to turn into right-handed circular polarization and vice versa in reflection. In other words, circu-

lar polarization cross-conversion needs to be small. This is equivalent to stating that the structures must not exhibit additional linear birefringence. This condition has not been fulfilled in Ref. [35], hence a chirality parameter could not be (and has not been) correctly retrieved.

More recent experimental work [42] has attempted to bring the structures of Ref. [33] (albeit with some modifications and simplifications) towards optical frequencies. Here, circular polarization conversion has been negligible and a maximum difference of the circular refractive indices of about 0.34 has been retrieved [42]. This difference is twice the chirality parameter. Both indices, however, have remained positive throughout the entire spectral range. Still, such structures are interesting and relevant as the optical activity obtained is rather broadband (about 100-nm bandwidth at around 1360-nm center wavelength) and many orders of magnitude larger than what is obtained from, e.g., solutions containing chiral sugar molecules [42].

4.2.6 On measurements of the effective refractive index

In order to somewhat justify the use of the *effective* refractive index, n, of metamaterials made of stacked layers of periodic inclusions, convergence of the retrieved value of n when increasing the number of layers has been studied experimentally in [12]. The observed convergence rate of n proved to be consistent with the findings of the theoretical paper [43] based on a similar double-fishnet type negative-index photonic metamaterial design. Ref. [43] reports convergence for four functional layers. However, one should be aware that these quantities are not the fundamental physical parameters at all. Increasing the spacing between adjacent functional layers of the double-fishnet structure will decrease their coupling (see discussion in Section 4.2.1). As a result, convergence can even be achieved for a single functional layer [44]. Inferring other optical parameters (e.g., permittivity or permeability) from such refraction experiments [12] again requires making reference to the dedicated theoretical models of the measured specimens.

An alternative type of the refraction measurements is based upon the use of prism made of wedge-shaped metamaterial sample (rather than the slabs discussed so far). The direction of the light wave transmitted through such samples generally changes due to refraction. Measuring the corresponding light deflection angles allows the refractive index to be inferred by applying Snell's law. However, such obtained refractive index is generally differ from the refractive index n usually referred to in connection with the phase velocity of light, c, in material being slower by factor n than the vacuum speed of light, c_0, i.e., $c = c_0/n$. A brief discussion of this aspect can be found, e.g., in Ref. [45]. The experiments addressing the change in the direction of the Poynting vector (energy flow) have been published [12]. The samples investigated in [12] were fabricated via evaporation of a stack of 21 alternating layers of silver and dielectric (corresponding to 10 lattice cells). Next, holes were drilled using focused-ion-beam (FIB) lithography to obtain a stacked fishnet type structure. Finally, a wedge which forms a prism has been produced, again using FIB lithography. The measured wavelength-dependent changes in beam direction have been compared with the time-domain simulations in CST Microwave Studio. The calculations agree regarding the real part of the refractive index, and the authors have concluded that ten functional layers (lattice cells) suffice for the retrieved

effective refractive index to be representative of the value for "bulk" material. However, the same calculations disagree with the experimental data by a factor larger than five for the imaginary part of the refractive index, i.e., the maximal measured figure of merit of about 3 is much smaller than the calculated value of about 20.

Different approach to retrieval of the metamaterial parameters has been presented in ref. [61]. The high-resolution spectral method based on Bloch-wave symmetry properties was applied experimentally to extracting mode dispersion in periodic waveguides. The technique is based upon the measurements and mapping of near-field profiles. Both the travelling and evanescent modes were taken into account, and the amplitudes of forward and backward waves in different waveguide configurations were determined with the estimated uncertainty of several percents or less. Whereas the commonly employed Spatial Fourier-Transform (SFT) analysis provides the wavenumber resolution which is limited by the inverse length of the waveguide, the precise dispersion characteristic extraction has been achieved even for compact photonic structures. While the measurement concept is generally applicable to arbitrary frequencies, the experimental results have been presented only in the microwave range. The examples of periodic dielectric waveguide, artificial transmission line and overmoded dielectric slab waveguide have illustrated robustness of the developed approach to retrieval of the dispersion characteristics by mapping the field distributions.

4.3 "Road map" for experimental characterization of complex electromagnetic materials

Recent advances in electromagnetics of complex materials and technological developments have enabled the design and fabrication of numerous new types of micro- and nanostructured artificial electromagnetic media. New electromagnetic phenomena observed in the novel inhomogeneous structures lead to new electromagnetic properties, which could enable new industrial applications. These properties may extend beyond those of natural materials or even be absolutely new.

To understand the properties of these new materials and evaluate the applicability of the structure to target applications one should first determine if a particular structure can be described by a few parameters characterizing **material** or the structure demonstrates so-called mesoscopic properties, i.e. properties that change from sample to **sample,** depending on its size, shape, and environment.

This "road map" gives some guidance on how one can experimentally determine what kind of structure we deal with and, if this is indeed a new **material,** how to assess the electromagnetic properties of composite material samples. This usually means measurement of effective material parameters, like permittivity and permeability tensors (sometimes also electromagnetic coupling tensor), which define the response of an effectively continuous material to the excitation by electromagnetic waves.

We assume that the sample of the composite material under characterization is shaped as a planar layer: a slab. The challenge is to determine experimentally if this material is an artificial dielectric or artificial magnetic or bianisotropic material, or it is a photonic crystal or something else. If possible, we should retrieve its material parameters from

measurement data.

Experimental steps	**Short explanations**
Step 1. Is the sample a piece of an effectively homogeneous material or a (complicated mesoscopic) structure?	
Measurement of diffuse scattering from the sample shaped as a planar layer. The sample is illuminated by a wave beam with nearly flat phase front incident at a certain angle. The beam width is small enough so that the edges of the layer under characterization are not illuminated. This incident wave beam models the plane wave incident on the infinitely extended layer. Amplitude of fields, reflected, transmitted and scattered at all directions, is measured. Measurements at a given frequency can be repeated for several incidence angles. These measurements can be done at several frequencies.	The aim is to determine the level of diffusion scattering for frequencies and angles of incidence which are of our interest. If we observe that (for a given frequency and incidence angle) nearly all reflected energy propagates in the specular direction, according to the usual reflection law, then we deal with an effectively homogeneous sample (for this frequency ω and this incidence angle α). If we observe side lobes or high level of diffusion scattering, it means that the sample is not an effectively homogeneous material, and we deal with a more complex system. This can be a diffraction grating or a photonic crystal or whatever.
If the level of diffusion scattering is small, we can pass to **Step 2.** Are the effects of spatial dispersion [62] weak or strong?	
Measurement of the plane-wave reflection R and transmission T coefficients of the sample at the given frequency 1) in a uniform medium and 2) stacked with a conventional material sample, for example, a dielectric layer (which is referred to as the *test layer*). The incident field is the same wave beam as in Step 1. First, we find from R and T coefficients the transmission matrix [63, 64] of the sample under test and the transmission matrix of the test layer separately. Next, we bring them together, measure the transmission matrix of the whole stack and compare it with the product of the two previously measured matrices.	If the sample under characterization is effectively homogeneous, the transfer matrix of the stack of two layers (the composite layer and the test layer) should be equal to the product of the transfer matrices of the two slabs. The exceptions from this rule refer to the case when the presence of the dielectric layer enhances the manifestation of the structure heterogeneity (for the wave in free space the structure behaves as an effectively continuous, but for the wave in the dielectric, as a discrete one). Then one has to take another dielectric layer with a smaller refraction index.

If we find out that the effective response of the sample does not change when we bring the sample close to a test sample (with the known properties), then the spatial dispersion is weak enough and we can pass to

Step 3. Search for the minimal set of local constitutive parameters

Study the polarization characteristics of reflected and transmitted waves at several incidence angles, using, for example, ellipsometry set-ups. Illumination from both sides is necessary to assess reciprocity and bi-anisotropy of the sample.	We determine the type of the material (isotropic, anisotropic, bianisotropic, chiral, gyrotropic) analyzing the polarization ellipses of the reflected and transmitted waves.

Step 4. Retrieval of local constitutive parameters

Using RT-retrieval (e.g., modern variants of the NRW technique [65, 66] and its extensions) or ellipsometry (note, however, that ellipsometry methods are well developed only for non-magnetic layers) determine the bulk effective material parameters. For RT-retrieval, measurements of both amplitude and phase of the reflection and transmission coefficients are necessary. If the material under characterization is prepared on a wafer or another substrate whose thickness is larger than that of the material layer under test, the substrate of the same thickness should be studied separately in order to measure the S-matrix of the material layer under test.	At this stage the numerical values of constitutive parameters are determined as functions of the frequency.

Step 5. Analysis of the retrieved parameters and interpretation of the results ("sanity check")	
Analyse the results. Elaborate methods of measurement of new (alternative) parameters, if that is necessary, and then make these new measurements. Repeat this analysis stage... until the results are satisfactory.	To analyze whether the obtained set of constitutive parameters makes physical sense and if these parameters can be indeed used to describe the material of the sample. One should check the following key issues: A. Energy conservation is not violated (the imaginary parts of the permittivity or permeability do not change signs and the real part of the effective impedance is positive) [62]. B. Constitutive parameters do not depend on the thickness or shape of the sample. C. Causality principle [62] is not violated - that is, the model does not allow any response before the corresponding stimulus has been applied. This can be confirmed from the analysis of the frequency dependence of the effective permittivity and permeability. For causal materials the real and imaginary parts of the material parameters satisfy the Kramers-Kronig relations [62], and in the low-loss regions and well below resonances the permittivity and permeability grow with increasing frequency) [62]. D. The retrieved parameters do not depend on the incidence angle and the sample thickness (otherwise they characterize not the material, but only this sample for this particular excitation).

If the above procedure successfully "converges", this means that the sample under test can be characterized by conventional (volumetric) effective parameters: permittivity, permeability, chirality parameter, etc. These parameters can be used in device design, because the parameters indeed describe the properties of the material, which will not change if the size or shape or position of the sample will be different than in the measurement

set-up. The theoretical background which is necessary for the analysis at the last step is briefly outlined in Section 3.3.1.

If this is not the case, the conclusion is that the retrieved material parameters have a limited validity region and, most likely, unconventional physical meaning. However, in studies of metamaterials compromises often have to be made, as in many instances there are no better ways to describe the "material" response than using these "material parameters". They can successfully provide some qualitative description of physical phenomena in the sample, but care should be taken in understanding the limitations for their use.

4.4 How to choose the appropriate measurement technique and equipment?

4.4.1 General considerations

When characterising a nanostructured materials sample, it is important that the appropriate technique and equipment is employed. Choosing unsuitable equipment, or indeed equipment that is not properly configured, is likely to cast doubt onto the validity of recorded measurements. What can be considered appropriate is primarily defined by two factors - the parameters being characterised and the type of nanostructured material under examination. Because there are such a wide and expansive variety of nanostructures, each of which has its own defining characteristics, there is no universal system configuration that can be used to successfully measure every type of sample. Certain materials may, for example, require incident light to be polarised, confined to a specific spectral range or have a variable angle of incidence whilst other samples will not require such conditions. Therefore it is essential that the person or persons performing the characterisation understand the appropriate measurement technique and the associated equipment to be used. Here we will discuss the considerations to be made when selecting a characterisation technique and the equipment needed at each step (see Section 4.3) to perform such measurements.

The initial step in the characterisation of a sample is its identification as either a homogeneous material or a mesoscopic structure. Complex mesoscopic structures do not display the same radiation scattering uniformity as homogeneous materials when appropriately measured [67]. Therefore the sample type can be distinguished using one of two techniques: diffuse scattering and transmission electron microscopy (TEM). While TEM can provide high resolution electron diffraction patterns for detailed observation of a multilayered sample [**?**], its one significant drawback is that it inherently damages the specimen under examination, rendering it useless for future steps. With respect to degree of importance, this is likely to supersede the advantage of spatial resolution of only a few AAngstroms and sensitivity to very weak scattering [69]. The non-destructive alternative is to take diffuse scattering measurements using a radiation beam with an appropriate wavelength for the sample. Depending on the apparatus used, incident waves scattered by the sample can be recorded to give either 2D or 3D image outputs. For 2D measurements, linear position sensitive detector (PSD) diffractometers are used to detect the scattered radiation over a range of diffraction angles (Figure 4.8). The PSDs

are arranged in an arc above the sample so that the scattered beams are incident normal to the detector window at all angles within the range of the diffractometer. Under this configuration, much of the scattered radiation is not detected and so valuable data that would be used to image a scatter pattern is lost. 3D outputs on the other hand can be retrieved using flat image plate (IP) detector systems that use higher incident waveform energies. An increase in energy results in better detection for highly absorptive samples and smaller angles of diffraction, meaning the detection process is easier and can be more extensive [70]. In both PSD and IP configurations, a monochromator and a collimator are affixed to the output of the beam generator, ensuring the incident waves are all normal to the sample and of a desired frequency. The collimator is generally positioned approximately two millimetres from the surface of the specimen and a beamstop, used to restrict the perpetual travel of the waveform, is placed about eight millimetres behind the sample [70]. Because the collimator and beamstop are placed so close to one another, air scattering is virtually eliminated. During the measurement process, the sample is scanned while it gradually rotates; for example 1000 scans at rotational increments of 0.36°. If the detectors were rotated instead, there would be a likelihood of unwanted vibrations distorting the measurement data.

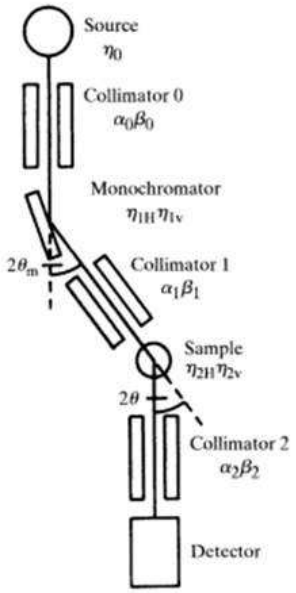

Figure 4.8: A schematic diagram of a diffractometer showing divergence at each stage of the measurement process [71].

An alternative to IP systems is that of charge coupled device (CCD) detection. CCD plates are usually smaller in size to image plates and so are placed much closer to the sample being measured to ensure sufficient retrieval of scattered radiation. Furthermore, adjustments and corrections have to be made for spatial distortions that are inherent in CCD detection. However with CCDs, measurements can be made and computed within a matter of seconds, unlike IP systems which take one or two minutes to output data [70]. Because of the more efficient use of time, the sample can be rotated in smaller increments, such as 0.1°, to give a more accurate representation of the specimen characteristics. A further advantage of CCD systems is that they can operate using incident waves at a

lower energy than alternative PSD and IP configurations.

Following identification of the sample, measurement of the broadband plane-wave transmission and reflectance spectra must be taken. This is the predominant characterisation method for optical metamaterials [72]. There are numerous ways to successfully retrieve the R and T coefficients of a sample, each of which utilizes different types of equipment. The most common commercial piece of apparatus for this purpose is a spectrophotometer which, as its name suggests, is an amalgamation of a spectrometer and photometer. The spectrometer part of the system outputs light of a selected wavelength at an incident angle to the sample under examination while the resultant radiant flux is measured by a photometer. Spectrophotometers commonly use two incident beams during R and T retrieval (one for measurement and the other for a reference) and allow the angle of incidence to be adjusted to suit requirements. However, whilst these systems are specifically manufactured for R and T measurement, they are in most cases not appropriate in the characterisation of metamaterials and nanostructures. This is because spectrophotometers require a comparatively large patterned area to measure and nanostructures fabricated using electron-beam lithography and other such protracted techniques typically cover an area no larger than a few square millimetres [6]. Nevertheless the principles of R and T retrieval with spectrophotometers can be adapted for use in a "custom built" apparatus setup, an example of which is shown in Figure 4.9.

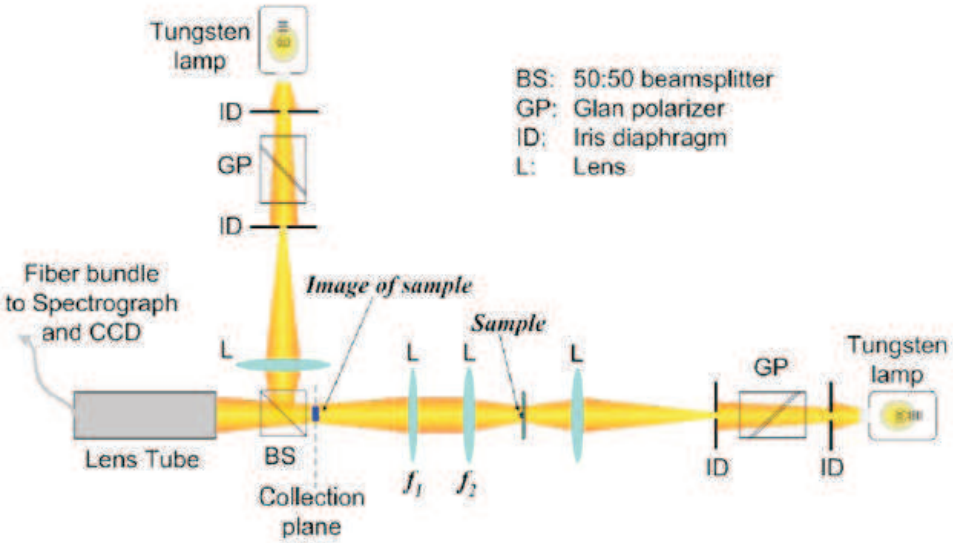

Figure 4.9: Experimental custom-built system for the retrieval of broadband transmission and reflection spectra of small samples [73].

Such a system may function by imaging the sample, through use of optical magnification, onto a spectrograph with polarised light. A reliable polariser such as a Glan-Taylor prism could be positioned in front of the light source to polarise the light to the desired linearity [72]. This is particularly important in the case of metamaterials, most of which are anisotropic. The incident light itself should be generated from a broadband source, for example a tungsten-halogen lamp. Beamsplitters, iris diaphragms and multiple lenses and mirrors are likely to be required in a custom built arrangement to restrict and control the light's direction of travel. In order to analyse the spectrum produced by the

lamp, a monochromator can be placed between the polariser and the sample. Placing the monochromator in the path of the reflected light (i.e. between the sample and the detector) allows selectivity of the reflectance spectra. Reference reflectance measurements can be taken using a clean, unblemished mirror while transmission references can be taken using either free space or an unpatterned area of the sample surface, depending on whether all layers or just the nanostructures are to be analysed [72].

Whilst it does not directly measure reflectance and transmission, Fourier transform infrared (FTIR) spectroscopy can provide values for both coefficients. FTIR, and indeed other types of interferometric spectroscopy, operate by splitting the incident beam using a partially reflective material [74]. The system, often configured in the Michelson arrangement, then creates interference between the original beam and one subjected to a longitudinal delay before being input to the detector [75]. The interferogram produced contains data from all wavelengths produced by the infrared light source with respect to time. Fourier transformation can then be performed on the output interferogram to give a calculated frequency spectrum. This is known as a time-domain measurement as the R and T spectra are not directly measured. Unlike systems with a monochromator, FTIR measures waves at all generated frequencies simultaneously, eliminating the need for multiple measurements and thus speeding up the process considerably. Additionally, because of the greater optical throughput, FTIR spectra also display a more desirable signal-to-noise (SNR) ratio than many dispersive spectrometers [72]. A further advantage of interferometric spectroscopy over dispersive methods is that often phase information can be determined, provided certain criterions are met [76]. The Mach-Zehnder interferometer configuration can be used as an alternative to the Michelson arrangement to determine the relative phase shift between the two beams. Unlike the Michelson system, Mach-Zehnder interferometers utilize two beam splitters to ensure that the split beams are not recombined and are measured using separate detectors. Because both beams are detected individually and neither one is reflected back into the source, as is the case in the Michelson configuration, disruptive interference as a result of intensity and phase modulation is prevented [77]. Furthermore, because both beams of light travel parallel to one another rather than orthogonally, the Mach-Zehnder system is more resilient to environmental disturbances than the Michelson interferometer [77].

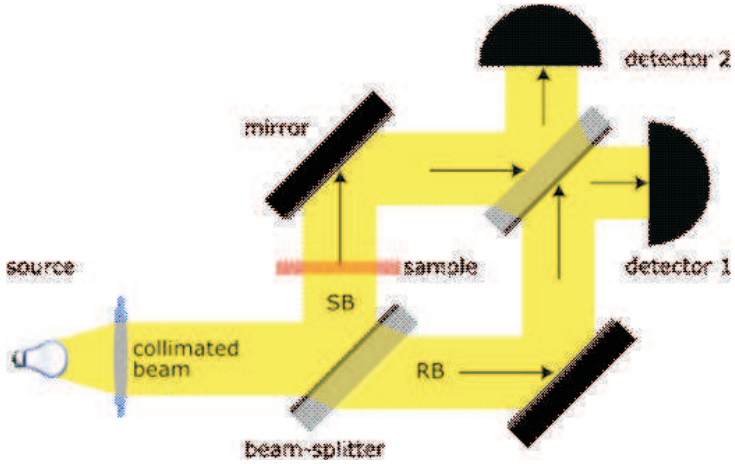

Figure 4.10: Diagram showing the path of light in a Mach-Zehnder interferometer [78].

Before measurements can be successfully taken, the variable phase shifters and attenuators in the system must be properly calibrated. This can be achieved by varying the optical path length in the case of the phase shift and subjecting the light to total internal reflection within two prisms for attenuation purposes [79]. With reference to figure 3, without a sample present both beams at detector 1 will have been reflected twice (once by a beam splitter and once by a mirror) and will have passed through the glass body of a beam splitter. Because there is no phase difference between the two waves in this instance, constructive interference will be present at detector 1. However, total destructive interference is present at detector 2 as the beams are half a wavelength out of phase with each other. This is due to differing optical path lengths and results in no light being detected. Therefore placement of a sample in the path of a beam changes the wave intensity and phase, creating the proper circumstances for measurement. Comparison of the data retrieved by both detectors allows calculation of the inherent phase shift of the sample being analysed. Adapted Mach-Zehnder interferometers have also been used to measure the refractive index of samples [80]. Irrespective of the interferometer used for characterisation, computer software is required for the purpose of executing the Fourier transforms on the produced interferogram to give the resultant frequency spectrum.

In order to find the minimal set of local constitutive parameters, the polarization characteristics of reflected and transmitted waves must be studied. This is done using non-destructive and contactless ellipsometry methods. Successful execution of this stage will determine the type of material under examination; for example whether it is isotropic, anisotropic, bi-anisotropic, chiral or gyrotropic. Ellipsometry techniques, of which there are many [81], measure the change in the polarization state of light reflected by the specimen from the light that was originally transmitted. The transmitted light, of which the intrinsic properties are known, is compared with the measured light reflected by the sample, thus allowing the change in polarisation to be analysed. By probing the complex refractive index or dielectric function tensor elemental physical properties such as morphology, crystal quality, chemical composition and electrical conductivity can be found [16]. Ellipsometry is most commonly used to characterise film thickness for either single layers or multilayer structures and to find the complex permittivity [82]. Typically, an ellipsometer will comprise of a light source, polariser, compensator, analyser and a detector. There are two primary categories of ellipsometers: rotating optical element systems and instruments with photoelastic modulators [81]. Systems with rotating elements are likely to have either a rotating analyser (rotating analyser ellipsometry, RAE) or a rotating compensator (rotating compensator ellipsometry, RCE), although other setups do exist [18]. Irrespective of the type of ellipsometer system used, it can be configured so that the reference wavelength, illumination angle and sample orientation can all be altered and varied. Antiquated systems use a monochromator to select the desired wavelength of incident light and a photomultiplier tube for detection [84]. However more efficient setups employ a white light source for the incident wave and a photodiode array as a detector, allowing simultaneous measurement of a broadband spectrum and a real-time display of the results [85]. The light, which is initially unpolarised, is transmitted through a polariser that is oriented between the p- and s-planes. It is then targeted onto the sample surface so that the linearly polarised light is reflected and becomes elliptically polarised before passing through an analyser which, depending on the system configuration, may or may not be rotating. The photodetector then converts the detected light into an electronic signal

for mathematical processing, performed using both the reference and reflected waveforms. The resultant complex polarization ratio, ρ, can then be calculated using the measured values of amplitude ratio and phase shift, denoted by Ψ and Δ, respectively. In the case of anisotropic multilayer thin films, as many as ten parameter measurements need to be made for each layer – nine for the dielectric tensor and one for film thickness [86]. These measurements must also be taken over a wide range of incident and azimuthal angles to ensure an adequate span of data is retrieved. Each individual dielectric tensor and thickness parameter should noticeably alter the detected polarisation data and not give a linear output of collated results [86]. By utilising a Mueller matrix, the dielectric tensor parameters can then be determined by the ellipsometer software. When selecting an ellipsometer configuration it may be worthwhile to consider some of their advantages and drawbacks. Both Rotating Polariser Ellipsometers (RPE) and RAEs are very accurate and easy to construct but their measurement of phase shift is less sensitive at 0° and 180°. RPE systems are likely to suffer from residual polarisation from the incident source wave [83]. In both systems the rotating element is likely to need calibration for the highest accuracy measurements to be obtained. RCE ellipsometers have the advantage of using two static polarisers that eliminate the problems caused by residual polarisation and can measure Ψ and Δ without suffering from a lack of sensitivity at certain values. Also worth consideration is the inclusion of a monochromator. As monochromators produce partially polarised light they are often placed after the sample, meaning a wide spectrum of white light is incident on the specimen [83]. This is of course important if the sample is in any way photosensitive. Following the retrieval of the polarization characteristics the numerical values of constitutive parameters can be deduced using the Nicholson-Ross-Weir (NRW) method for completion of the characterisation. No experimental equipment is needed for this stage but commercial software is available for the convenient calculation of parameter values.

4.5 Measurement equipment needed for electromagnetic characterization of materials

The web site of the ECONAM project (Coordination Support Action funded by the European Commission within FP7 NMP priority area contains an extensive list of relevant measurement equipment types as well as links to the European institutions which have such installations and expertise in making necessary measurements.

The web site can be found at the address

http://econam.metamorphose-vi.org/

4.6 Concluding remarks

Optical metamaterials, because of their typically limited area and number of functional layers, are more easily understood as finite structures with interfaces that define their optical behaviour. This definition is in contrast to a conventional material in which their bulk properties define their optical properties. The retrieved 'material' parameters are

the subject of interpretation unless the samples have sufficient extent in the measurement direction to suppress the interface effects. Also the phase information is harder to obtain giving the need for either more sophisticated measuring tools, such as time domain or interference methods, or alternatively, more complex structures, i.e. phase masks made with the metamaterial.

The current challenges and difficulties of characterization of nanostructured materials have been summarised in [47] where the author stated that "... as we near the one hundred year mark since the birth of crystallography, we face a resilient frontier in condensed matter physics: our inability to routinely and robustly determine the structure of complex nanostructured and amorphous materials. Yet what has become clear with the emergence of nanotechnology is that diffraction data alone may not be enough to uniquely solve the structure of nanomaterials". Commenting on the recent paper [48] which presented the approach to determination of the structure of complex nanostructured materials, the author argued that the major challenges arise from the limited information content of the measurement data along with the growing complexity of the models used for data post-processing. Uniqueness of the associated inverse problems is a real issue, as is the availability of good nanostructure solution algorithms. Additional constraints coming from prior knowledge about the system, or additional data sets, from different information sources are required to constrain a unique solution for retrieval of the material parameters. The author of [47] suggests: "We may be relearning lessons from crystallography... These constraints are just common sense, but place enormous restrictions on the solution space and the efficiency and uniqueness of solutions. Nanostructure solution is much younger than crystallography, but the field is rapidly growing up."

Bibliography

[1] V.M. Shalaev, Nature Photon. 1, 41 (2007).

[2] C.M. Soukoulis, S. Linden, and M. Wegener, Science 315, 47 (2007).

[3] K. Busch, G. von Freymann, S. Linden, S. Mingaleev, L. Tkeshelashvili, and M. Wegener, Phys. Rep. 444, 101 (2007).

[4] S. Zhang, W. Fan, N.C. Panoiu, K.J. Malloy, R.M. Osgood, and S.R.J. Brueck, Phys. Rev. Lett. 95, 137404 (2005).

[5] N. Feth, C. Enkrich, M. Wegener, and S. Linden, Opt. Express 15, 501 (2007)

[6] W. Wu, E. Kim, E. Ponizovskaya, Z. Liu, Z. Yu, N. Fang, Y.R. Shen, A.M. Bratkovsky, W. Tong, C. Sun, X. Zhang, S.-Y. Wang and R.S. Williams, Appl. Phys. A 87, 143 (2007).

[7] Jin Hyoung Lee, Qi Wu, and Wounjhang Park, Metal nanocluster metamaterial fabricated by the colloidal self-assembly, Optics Letters, Vol. 34, Issue 4, pp. 443-445 (2009)

[8] Jonathan A. Fan, Chihhui Wu, Kui Bao, Jiming Bao, Rizia Bardhan, Naomi J. Halas, Vinothan N. Manoharan, Peter Nordlander, Gennady Shvets, Federico Capasso, Self-Assembled Plasmonic Nanoparticle Clusters, Science, Vol. 328. no. 5982, pp. 1135 - 1138, May 2010.

[9] Kristof Lodewijks, Niels Verellen, Willem Van Roy, Gustaaf Borghs, Pol Van Dorpe, Self-assembled hexagonal double fishnets as negative index materials, Preprint arXiv:1010.5138v1, Oct. 2010.

[10] G. Dolling, M. Wegener, and S. Linden, Opt. Lett. 32, 551 (2007).

[11] N. Liu, H. Guo, L. Fu, S. Kaiser, H. Schweizer, and H. Giessen, Nature Mater. 7, 317 (2008).

[12] J. Valentine, S. Zhang, T. Zentgraf, E. Ulin-Avila, D. A. Genov, G. Bartal, X. Zhang, Nature, 455, 376 (2008); doi:10.1038/nature07247.

[13] S. Warren, Science (2008) vol. 320, 1748

[14] W. Zhang et al., J. Opt. A: Pure Appl. Opt. (2006) vol. 8, 878

[15] H.J. Lezec, J.A. Dionne, and H. Atwater, Science 316, 430 (2007).

[16] Nanostructured Metamaterials, Exchange between experts in electromagnetics and materials science, Ed Anne F de Baas, Luxembourg, European Union 2010, ISBN 978-92-79-07563-6

[17] `http://en.wikipedia.org/wiki/Fourier_transform_infrared_spectroscopy`, consulted 13.10.2010

[18] `http://en.wikipedia.org/wiki/File:Ellipsometry_setup.svg`, consulted 13.10.2010

[19] Novel Techniques in THz-Time-Domain-Spectroscopy, A comprehensive study of technical improvements to THz-TDS Matthias Hofmann Inaugural-Dissertation Fakultät für Mathematik und Physik der Albert-Ludwigs-Universität Freiburg im Breisgau vorgelegt von Stefan Gorenflo aus Hausen im Wiesental im November 2006 (see Chapter 3).

[20] E. Pshenay-Severin, F. Setzpfandt, C. Helgert, U. Hbner, C. Menzel, A. Chipouline, C. Rockstuhl, A. Tnnermann, F. Lederer, and T. Pertsch J. Opt. Soc. Am. B, 27, No. 4/ pp 660-666 April 2010.

[21] Jiaguang Han, "Probing negative refractive index of metamaterials by terahertz time-domain spectroscopy", Optics Express, 16, no. 2, pp. 1354 - 1364 (2008).

[22] Ugur Cem Hasar "A Generalized Formulation for Permittivity Extraction of Low-to-High-Loss Materials From Transmission Measurement", IEEE Trans. on Microwave Theory and Techniques, 58, 2, pp. 411-418, Feb. 2010.

[23] Ugur Cem Hasar, "Accurate Complex Permittivity Inversion From Measurements of a Sample Partially Filling a Waveguide Aperture", IEEE Trans. on Microwave Theory and Techniques, 58, 2, pp. 451 - 457, Feb. 2010.

[24] M.S. Rill, C. Plet, M. Thiel, I. Staude, G. von Freymann, S. Linden, and M. Wegener, Nature Mater. 7, 543 (2008).

[25] A.R. Bungay, Yu.P. Svirko, and N. Zheludev, Phys. Rev. B 47, 11730 (1993).

[26] V.M. Shalaev, W. Cai, U.K. Chettiar, H. Yuan, A.K. Sarychev, V.P. Drachev, and A.V. Kildishev, Opt. Lett. 30, 3356 (2005).

[27] G. Dolling, C. Enkrich, M. Wegener, C.M. Soukoulis, and S. Linden, Science 312, 892 (2006).

[28] G. Dolling, M. Wegener, C.M. Soukoulis, and S. Linden, Opt. Lett. 32, 53 (2007).

[29] C. Enkrich, M. Wegener, S. Linden, S. Burger, L. Zschiedrich, F. Schmidt, J. Zhou, T. Koschny, and C.M. Soukoulis, Phys. Rev. Lett. 95, 203901 (2005).

[30] G. Dolling, M. Wegener, A. Schädle, S. Burger, S. Linden, Appl.Phys.Lett. 89, 231118 (2006).

[31] R. Marqus, F. Medina, and R. Rafii-El-Idrissi, Phys. Rev. B 65, 144440 (2002).

[32] X. Chen, B.-I. Wu, J.A. Kong, and T.M. Grzegorczyk, Phys. Rev. E 71, 046610 (2005).

[33] E. Plum, J. Zhou, J. Dong, V. A. Fedotov, T. Koschny, C. M. Soukoulis and N. I. Zheludev, Phys. Rev. B 79, 035407 (2009)

[34] S. Zhang, Y.-S. Park, J. Li, X. Lu, W. Zhang, X. Zhang, Phys. Rev. Lett. 102, 023901 (2009)

[35] N. Liu, H. Liu, S. Zhu, and H. Giessen, Nature Photon. 3, 157 (2009)

[36] I.V. Lindell, A.H. Sihvola, S.A. Tretyakov, A.J. Viitanen, Electromagnetic waves in chiral and bi-isotropic media, Norwood, MA: Artech House, 1994.

[37] D.H. Kwon, D. H. Werner, A. V. Kildishev, and V. M. Shalaev, Opt. Express 16, 11822 (2008)

[38] M. Wegener and S. Linden, Physics 2, 3 (2009)

[39] B.V. Bokut', V.V. Gvozdev, A.N. Serdyukov, Special waves in naturally gyrotropic media, *Journal of Applied Spectroscopy,* vol. 34, pp. 701-706, 1981.

[40] S. Tretyakov, I. Nefedov, A. Sihvola, S. Maslovski, C. Simovski, Waves and energy in chiral nihility, *Journal of Electromagnetic Waves and Applications,* vol. 17, no. 5, pp. 695-706, 2003.

[41] J. Pendry, A Chiral route to negative refraction, *Science,* vol. 306, pp. 1353-1955, 2004.

[42] M. Decker, M. Ruther, C. Kriegler, J. Zhou, C. M. Soukoulis, S. Linden, and M. Wegener, Opt. Lett., submitted (2009)

[43] C. Rockstuhl, T. Paul, F. Lederer, T. Pertsch, T. Zentgraf, T. P. Meyrath, and H. Giessen, Phys. Rev. B 77, 035126 (2008)

[44] C.M. Soukoulis et al., unpublished (2008)

[45] M. Wegener, G. Dolling, and S. Linden, Nature Mater. 6, 475 (2007).

[46] A. A. Sukhorukov, Sangwoo Ha, I. V. Shadrivov, D. A. Powell, and Y. S. Kivshar, Opt. Express 17, 3716 (2009)

[47] S.J.L. Billinge, "The nanostructure problem" Physics 3, 25 (2010), DOI: 10.1103/Physics.3.25

[48] M. J. Cliffe, M. T. Dove, D. A. Drabold, and A. L. Goodwin, "Structure Determination of Disordered Materials from Diffraction Data", Phys. Rev. Lett. 104, 125501 (2010)

[49] S. Burgos, R. de Waele, A. Polman, H. Atwater, Nature Materials 9, 407-412 (2010)

[50] M. W. Klein, C. Enkrich, M. Wegener, C. M. Soukoulis, and S. Linden, Single-slit split-ring resonators at optical frequencies: limits of size scaling, Opt. Lett. 31(9), 12591261 (2006)

[51] F. Hesmer, E. Tatartschuk, O. Zhuromskyy, A. A. Radkovskaya, M. Shamonin, T. Hao, C. J. Stevens, G. Faulkner, D. J. Edwards, and E. Shamonina, Coupling mechanisms for split ring resonators: Theory and experiment, Phys. Status Solidi 244(4), 11701175 (2007)

[52] N. Liu, S. Kaiser, and H. Giessen, Magnetoinductive and Electroinductive Coupling in Plasmonic Metamaterial Molecules, Adv. Mater. 20(23), 45214525 (2008)

[53] S. Ha, A. A. Sukhorukov, K.B. Dossou, L.C. Botten, C. Martijn de Sterke, and Y.S. Kivshar, Bloch-mode extraction from near-field data in periodic waveguides, Opt. Lett. 34, 3776-3778 (2009)

[54] N. Feth, M. Konig, M. Husnick, K. Stannigel, J. Niegemann, K. Busch, M. Wegener, S. Linden, Optics Express 18(7), 6545, 2010

[55] A. Arbouet, D. Christofilos, N. Del Fatti, F. Vallee, J Huntzinger, L. Arnaud, P. Billaud, M. Broyer, Phys. Rev. Lett. 93(12), 127401, 2004

[56] A. Bitzer, H. Merbold, A. Thoman, T. Feurer, H. Helm, and M. Walther, Terahertz near-field imaging of electric and magnetic resonances of a planar metamaterials, Optics Express, Vol. 17, Issue 5, pp. 3826-3834, 2009

[57] M. Burresi, D. van Oosten, T. Kampfrath, H. Schoenmaker, R. Heideman, A. Leinse, and L. Kuipers, Probing the Magnetic Field of Light at Optical Frequencies, Science 23 October 2009: 326 (5952), 550-553.

[58] D. Diessel, M. Decker, S. Linden, and M. Wegener, Near-field optical experiments on low-symmetry split-ring-resonator arrays, Optics Letters, Vol. 35, Issue 21, pp. 3661-3663, 2010.

[59] A. Liu, A. Rahmani, G. W. Bryant, L.J. Richter, and S.J. Stranick, Modeling illumination-mode near-field optical microscopy of Au nanoparticles, JOSA A, Vol. 18, Issue 3, pp. 704-716, 2001.

[60] D.H. Kwon, D. H. Werner, A. V. Kildishev, and V. M. Shalaev, Opt. Express 16, 11822 (2008)

[61] A. A. Sukhorukov, Sangwoo Ha, I. V. Shadrivov, D. A. Powell, and Y. S. Kivshar, Opt. Express 17, 3716 (2009)

[62] L.D. Landau and E.M. Lifshitz, *Electrodynamics of continuous media,* Pergamon Press, Oxford, 1960.

[63] D.M. Pozar, *Microwave Engineering,* Wiley, 1996.

[64] R.E. Collin, *Foundations for Microwave Engineering,* Mc-Graw Hill, New York, 1966 (first edition); 1992 (second edition).

[65] A.M. Nicolson and G.F. Ross, *IEEE Trans. Instrum. Meas.*, **17** (1968) 395.

[66] W.W. Weir, *Proc. IEEE*, **62** (1974) 33.

[67] van Rossum, Nieuwenhuizen, Multiple scattering of classical waves: microscopy, mesoscopy, and diffusion, Rev. Mod. Phys. 71, 313, 1999.

[68] Yamani, Gurdal, Alaql, Nayfeh, Correlation of diffuse scattering with nanocrystallite size in porous silicon using transmission microscopy, Journal of Applied Physics, 1999

[69] Barabash, Turci, Diffuse Scattering and the Fundamental Properties of Materials, Momentum Press, 2009

[70] Welberry, Diffuse X-ray scattering and models of disorder, International Union of Crysallography, Oxford University Press, 2004.

[71] Shmueli, International tables for crystallography, Volume 2, Third edition, Springer, 2008.

[72] Cai, Shalev, Optical Metamaterials: Fundamentals and Applications, 1st Edition, Springer, New York, 2010.

[73] Cai et al, Metamagnetics with rainbow colors, Optics Express, Vol. 15 No. 6, 3333, 2007.

[74] Brady, Optical imaging and spectroscopy, John Wiley & Sons and The Optical Society of America, 2009.

[75] Thorne, Litzen, Johansson, Spectrophysics: Principles and Applications, Springer, 1999.

[76] Dolling, Enkrich, Wegener, Soukoulis, Linden, Simultaneous Negative Phase and Group Velocity of Light in a Metamaterial, Science 312, 892, 2006

[77] Shamir, Optical Systems and processes, SPIE, Washington, 1999.

[78] http://en.wikipedia.org/wiki/Mach-Zehnder-interferometer, consulted 25/01/2011

[79] Edited: Palik et al, Handbook of Optical constants of solids, Vol. 4, Academic Press, 1998

[80] Schubert, Kuck, Gottfried-Gottfried, Refractive-index measurements using an integrated Mach-Zehnder interferometer, Sensors and Actuators A: Physical, Vol. 60, 108-112, 1997.

[81] Fujiwara, Spectroscopic Ellipsometry: Principles and applications, John Wiley & Sons, 2007.

[82] G. E. Jellison, Generalized ellipsometry for material characterization, Thin Solid Films 450 (2004) 42.

[83] J. A. Woollam, B. Johs, C. Herzinger, J. Hilfiker, R. Synowicki, and C. Bungay, Overview of Variable Angle Spectroscopic Ellipsometry (VASE), Part I: Basic Theory and Typical Applications, SPIE Proceedings, CR72, (1999) 3-28.

[84] Collins, Automatic rotating element ellipsometers: Calibration, operation and real-time applications, Rev. Sci. Instrum. 61, 2029, 1990.

[85] An, Li, Nguyen, Collins, Spectroscopic ellipsometery on the millisecond time scale for real-time investigations of thin-film and surface phenomena, Rev. Sci. Instrum. 63, 3842, 1992.

[86] Bass, Handbook of Optics, MacGraw-Hill, USA, 2010.